View metadata, citation and similar papers at core.ac.uk

brought to you by CORE

provided by AUC Knowledge Fountain (American Univ. in Cairo)

American University in Cairo

AUC Knowledge Fountain

Theses and Dissertations

2-1-2014

Some MIMO applications in cognitive radio networks

Feeby Magdy Girgis Salib

Follow this and additional works at: https://fount.aucegypt.edu/etds

Recommended Citation

APA Citation

Salib, F. (2014).*Some MIMO applications in cognitive radio networks* [Master's thesis, the American University in Cairo]. AUC Knowledge Fountain.
https://fount.aucegypt.edu/etds/1241

MLA Citation

Salib, Feeby Magdy Girgis. *Some MIMO applications in cognitive radio networks*. 2014. American University in Cairo, Master's thesis. *AUC Knowledge Fountain*.
https://fount.aucegypt.edu/etds/1241

This Thesis is brought to you for free and open access by AUC Knowledge Fountain. It has been accepted for inclusion in Theses and Dissertations by an authorized administrator of AUC Knowledge Fountain. For more information, please contact mark.muehlhaeusler@aucegypt.edu.

A-PDF Merger DEMO : Purchase from www.A-PDF.com to remove the watermark

The American University in Cairo

School of Sciences and Engineering

Some MIMO Applications in Cognitive Radio Networks

A Thesis Submitted to

The Electronics Engineering Department
in partial fulfillment of the requirements for
the degree of Master of Science

by Feeby Magdy Girgis Salib

under the supervision of Dr. Karim G. Seddik

July 2013

DEDICATION

I dedicate this thesis to God, and I thank Him for all His gifts and paving my way until I reached this point; I believe that He will continue paving my way and He will never leave me alone in my whole life.

I also dedicate this thesis to my lovely mother and my lovely father who always sacrifice with everything just to see me happy; and without their guidance and believing in me, I would have achieved nothing.

Moreover, I would like to dedicate this thesis to my advisor Dr. Karim G. Seddik who always supported me in my thesis research work; I would like to express my high appreciation and sincere gratitude to him for supporting me with motivation and encouragement.

ACKNOWLEDGMENTS

First and foremost, I acknowledge and thank God for all His blessings. Without His standing by my side I can do nothing.

I would like to acknowledge my advisor Dr. Karim Seddik for his endless patience, support and help. I would like also to thank him for his encouragement, motivation and guidance throughout my thesis work and academic study.

Moreover, I would like to acknowledge and thank my examiners, Prof. Dr. Hassanien Amer and Dr. Ahmed Ibrahim.

Also, I would like to acknowledge all my professors, especially my professor Dr. Ayman Elezabi. He was pushing me forward, and he always tried to give me self confidence since the first day I entered the Master's program.

I also want to acknowledge my professor Ms. Carol Clark who was my teacher in the English writing module; of course, without me being one of her students, I would not be able to write this thesis.

Last but not least, I would like to acknowledge all my friends and colleagues, especially my friend Afaf Ramzy and my colleague Mohamed Eissa, who always supported me and kept encouraging me. Also, I would like to send special thanks to Ms. Gehan. Moreover, special thanks go to my English teacher Ms. Mona Wilson who helped me so much in the preparation for the English entrance examination to the AUC.

A-PDF OFFICE TO PDF DEMO: Purchase from www.A-PDF.com to remove the watermark

ABSTRACT

The American University in Cairo, Egypt

Some MIMO Applications in Cognitive Radio Networks

Name: Feeby Magdy Girgis Salib

Supervisor: Dr. Karim G. Seddik

In the last decade, the wireless communication technology has witnessed a rapid development, which led to a rapid growth in wireless applications and services. However, the radio spectrum resources scarcity resulting from using the traditional methods of fixed spectrum resources allocation has potential constraints on this wireless services rapid growth. Consequently, cognitive radio has been emerged as a possible solution for alleviating this spectrum scarcity problem by employing dynamic resource allocation strategies in order to utilize the available spectrum in a more efficient way so that finding opportunities for new wireless application services could be achieved.

In cognitive radio networks, the radio spectrum resources utilization is improved by allowing unlicensed users, known as secondary users, to share the spectrum with licensed users, known as primary users, as long as this sharing do not induce harmful interference on the primary users, which completely entitled to utilize the spectrum.

Motivated by MIMO techniques that have been used in practical systems as a means for high data rate transmission and a source for spatial diversity, and by its ease implementation with OFDM, different issues in multi-user MIMO (MU-MIMO) in both the uplink and downlink in the context of cognitive radio are studied in this thesis.

More specifically, in the first thrust of this thesis, the spectrum spatial holes which could exist in an uplink MU-MIMO cell as a result of the possible free spatial dimensions resulted from the sparse activity of the primary users is studied; a modified sensing algorithm for these spectrum spatial holes that exploit both the block structure of the OFDM signals and the correlation of their activity states along time are proposed.

The second thrust is concerned with cognitive radio relaying in the physical layer where the cognitive radio base station (CBS) relays the PU signal while transmitting its own signals to its SUs. We define secondary users with different priorities (different quality of service requirements); the different levels of priority for SUs are achieved by a newly proposed simple linear scheme based on zero forcing called *Hierarchal Priority Zero Forcing scheme* HPZF.

TABLE OF CONTENTS

ABSTRACT **1**

LIST OF FIGURES **6**

LIST OF ABBREVIATIONS **8**

CHAPTER 1: BACKGROUND **9**

1.1 Cognitive radio 9

1.1.1 Multi-Dimensional Spectrum Opportunities 11

1.1.2 Cognitive radio System Architecture 11

1.2 OFDM 11

1.3 Muti-input Multi-output (MIMO) Systems 13

1.4 Compressive Sensing Background 14

1.4.1 $\ell 1$ and $\ell 2$ regularization 14

1.4.2 Compressive sensing 16

1.4.3 Block Sparse Reconstruction 17

CHAPTER 2: EXPLOITING SPATIAL SPECTRUM HOLES in MULTIUSER MIMO SYSTEMS **18**

2.1 INTRODUCTION 18

2.2 System Model 20

2.2.1 Primary User Network 20

2.2.2 Secondary User Network 21

2.3 SENSING STRATEGY 22

2.3.1 Static Environment 22

2.3.2 Dynamic Environment 24

2.4 Summary of the proposed algorithm 25

2.5 Simulation Results 25

2.6 Conclusion 27

CHAPTER 3: HIERARCHAL PRIOR ZERO FORCING for COGNITIVE RADIO NETWORKS 28

3.1 Introduction 28

3.2 System Model 30

3.3 Zero Forcing with different levels of priority 31

3.4 Hierarchal Prior Zero Forcing Analysis 32

3.4.1 Beamforming Vectors and Effective Channel Gains Calculations 33

3.4.2 Required Transmit Power 37

3.5 Comparing the different schemes 38

3.5.1 Comparison between HPZF and PZF 38

3.5.2 Comparison between HPZF and CZF 38

3.6 Special Case 39

3.6.1 Comparison between HPZF and PZF 41

3.6.2 Comparison between HPZF and CZF 42

3.6.3 Comparison between PZF and CZF [30] 43

3.7 Simulation Results and discussion 44

3.7.1 Total Required Power 44

3.7.2 Outage Performance 50

3.8 Results Summary 57

CHAPTER 4: CONCLUSION AND FUTURE WORK 58

4.1 Conclusion 58

4.2 Future Work 59

REFERENCES 60

LIST OF FIGURES

Fig. 1. 1 Cognitive radio system architecture 11

Fig. 1. 2 OFDM architecture 12

Fig. 2. 1 System Model 20

Fig. 2.2 Markov chain model of the PU activity 24

Fig. 2.3 4 QAM 26

Fig. 2.4 16 QAM 27

Fig. 3.1 Comparison of the required transmit power: M=2, L=3, 4, $R_p = R_{s1} = R_{s2}$ 45

Fig. 3.2 Comparison of the required transmit power: M=2, L=3, 4, $R_p = 1,\ R_{s1} = R_{s2}$ 45

Fig. 3.3 Comparison of the required transmit power: M=2, L=5, $R_p = 2,\ R_{s1} = 1.5$ 46

Fig. 3. 4 Comparison of the required transmit power: M=2, L=5, $R_p = 1.5,\ R_{s1} = 2$ 47

Fig. 3.5 Comparison of the required transmit power: M=2, L=5, $R_p = 1.5,\ R_{s1} = 0.5$ 47

Fig. 3.6 CBS-PU channel variance effect, M=2,L=3 48

Fig. 3.7 CBS-1st SU channel variance effect, M=2, L=3 49

Fig. 3.8 CBS- Varying both CBS-1st SU and CBS-PU channels variances, M=2, L=3 49

Fig. 3.9 Total required transmit power against both R_p and R_{s1}, L=3, M=2, $R_{s2} = 1$ 50

Fig. 3.10 Outage performance of the PU, M=2, L=4 52

Fig. 3.11 Outage performance of the 1st SU, M=2, L=4 53

Fig. 3.12 Outage performance of the 2nd SU, M=2, L=4 54

Fig. 3.13 Outage performance of the PU, M=3, L=4 54

Fig. 3.14 Outage performance of the 1st SU, M=3, L=4 55

Fig. 3.15 Outage performance of the 2nd SU, M=2, L=4 55

Fig. 3.16 Outage performance of the 3nd SU, M=3, L=4 56

Fig. 3.17 Comparison of the required transmit power: M=4, L=5, all SUs have the same target rates, $R_1 = 1$ 57

LIST OF ABBREVIATIONS

CBS	Cognitive Radio Base Station
CR	Cognitive Radio
CRN	Cognitive Radio Network
CS	Compressive Sensing
CZF	Conventional Zero Forcing
DSA	Dynamic Spectrum Allocation
FSA	Fixed Spectrum Allocation
HPZF	Hierarchal Prior Zero Forcing
LASSO	Least Absolute Selection and Shrinkage Operator
LS	Least Square
MAC	Multiple Access Control
MIMO	Multi Input Multi Input
MU	Multi User
MRT	Maximum Ratio Transmission
OFDM	Orthogonal Frequency Division Multiplexing
OSA	Opportunistic Spectrum Access
PBS	Primary Base Station
PU	Primary User
PZF	Prior Zero Forcing
QoS	Quality of Service
SINR	Signal to Interference plus Noise Ratio
SNR	Signal to Noise Ratio
SU	Secondary User
ZF	Zero Forcing

CHAPTER 1
BACKGROUND

In this chapter, the background concepts of cognitive radio system are presented followed a brief survey on multi-dimensional spectrum opportunities work existing in the literature. An overview of OFDM and MIMO systems are presented. Thereafter, the main concepts of ℓ_1- and ℓ_2-regularization are given, followed by a brief explanation of compressive sensing theory.

1.1 COGNITIVE RADIO

There has been a rapid growth in wireless communication applications and services including mobile communications, Wi-Fi, TV broadcast services, wireless PANs/LANs/MANs, etc. With this enormous development in the telecommunication field there is an increasing demand for wireless radio spectrum. Traditional methods for spectrum resources allocation assigns fixed frequency bands to licensed users. With this static assignment for the frequency bands, frequency regulatory bodies find themselves having spectrum shortage problem for providing new services. However, according to a recent study by the Federal Communications Commission (FFC), 90% of most of the fixedly assigned bands capacity is not utilized [1] due to the rare utilization of the licensed holders to their spectrum, leading to virtual spectrum scarcity. Consequently, traditional methods of the resource spectrum allocation have been proven to be an inefficient way for utilizing the available spectrum resources. Therefore, new policies should be developed to utilize these scarce spectrum resources in a more efficient way.

Cognitive radio has emerged as a promising solution for the spectrum scarcity problem. Unlike the traditional static allocation paradigms, cognitive radio technology allocates spectrum bands dynamically alleviating the inefficient use of the available spectrum recourses. In cognitive radio networks *Dynamic Spectrum Allocation*(DSA) policy is adopted instead of the *Fixed Spectrum Allocation* (FSA) policy, where unlicensed users known as secondary users SUs are allowed to utilize the spectrum allocated for the licensed users known as primary users PUs without causing interference to these PUs, which have the absolute priority. For SUs to be allowed for utilizing the spectrum they have to adapt their

transmissions according to primary users' usage for their licensed spectrum, while PUs are entitled to use the spectrum whenever they need. There are two main models in the literature where a CR can utilize the radio spectrum [2]; concurrent spectrum access model or underlay spectrum sharing model [2], [3] is a model where SUs are allowed to transmit data simultaneously with PUs unless they do not violate a predetermined noise interference temperature limit. Opportunistic spectrum access (OSA) model or overlay sharing model [2], [3] where SUs are allowed to access portions of the spectrum only when PU is not using them, which known as spectrum holes. If the SUs are under the OSA model, they have to monitor the activity of the PU so that they can vacate the spectrum once the PU reappear. This monitoring is done via spectrum sensing, which is the main task of a cognitive radio. In this thesis, we will consider the OSA model in the context of multi-user MIMO (MU-MIMO).

The most crucial function of a CR is to sense its surrounding environment so that it can monitor the PU behavior in order to adapt its utilization of the radio spectrum according to the PUs activity. In the OSA model, CR has to sense the spectrum to discover the spectrum holes, upon which the CR can adaptively assign these free spectrum holes to prospective secondary users. Different spectrum sensing techniques have been developed to sense these spectrum holes [4][5]. Energy detector is a simple technique where the received signal energy is measured and compared to a threshold that depends on the noise floor. Matched filter detector known as the optimum detector is another sensing technique that demands the knowledge of the PU signaling features and correlates the received signal to decide if it belongs to the PU or not. Another sensing technique is the cyclostationary-based sensing detector, which exploits the cyclostationarity of PU signals so that the differentiation between a pure noise signal and a PU's signal could be done.

Since the two main resources in wireless communications are the energy and bandwidth, CR technology enables efficient and flexible utilization of these limited communication resources. Therefore, a CR has cognitive capability and cognitive reconfigurability [4]. Cognitive capability means to have the ability to get the knowledge and the information about the surrounding environment and users needs, which is dependent on the spectrum sensing, while cognitive reconfigurability is how to achieve optimal performance through making the strategies for spectrum allocation and management according to the gathered information about the surrounding environment variations.

1.1.1 Multi-Dimensional Spectrum Opportunities

The traditional concept is that a spectrum opportunity exists when the PU is not using a band of frequencies at certain duration of time in a certain geographical space [6]. As a result, the dimensions of spectrum that have been studied in the literature in the context of CR are frequency, time and space [6]. Few papers explored other spectrum dimensions such as the code and angle dimensions. When spread spectrum techniques such as Direct Sequence Spread Spectrum or Frequency Hopping Spread Spectrum deployed, there could be opportunities of spectrum sharing that traditional spectrum sensing methods fall to detect [5]. Also, many researchers [7] tried to use beamforming to create new spectrum sharing opportunities rather than the traditional ones by using muti-antenna technologies, but at the expense of more complex techniques that requires estimating the channel on the link between the CR transmitter and PU receiver, which needs some collaboration from the PU side.

1.1.2 Cognitive radio System Architecture

A CR requires a cross-layer design to enhance spectrum efficiency [8].A simple architecture of a CR is shown in Fig. 1.1. A CR will have the usual PHY and MAC Layers and a Cognitive Layer that learns the medium, adapts to it and reconfigures the CR unit.

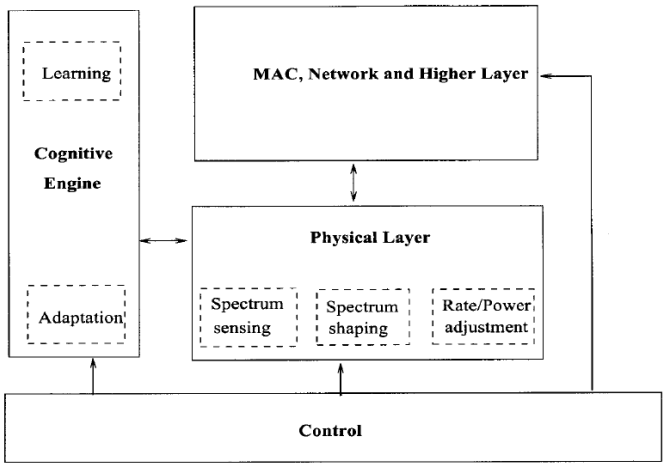

Fig. 1. 1Cognitive radio system architecture [7]

1.2 OFDM [9][10]

Orthogonal frequency division multiplexing (OFDM) is a multicarrier modulation technique that has become popular for high data rate wireless communication. It has been

considered as an attractive modulation technique due to its various advantages. It converts frequency selective fading channel into a number of flat fading sub-channels, hence, the equalization at the receiver is simplified. OFDM efficiently utilize the spectrum bandwidth since it permits overlapping between subcarriers in the frequency domain while orthogonality between subcarriers is maintained in the time domain.

The idea behind OFDM is to split the data symbols stream into many parallel lower rate streams and transmit the parallel streams on orthogonal subcarriers; therefore the duration of each symbol increases, hence, the wide band selective fading channel is divided into many narrow band flat fading subchannels. Using orthogonal overlapping subchannels makes OFDM a bandwidth efficient modulation technique. In OFDM, the intersymbol interference that could exist as a result of time dispersive channels can be canceled by using the Cyclic Prefix (CP), which is a copy of the last part of the OFDM symbol that is added to the beginning of that symbol. The architecture of OFDM system can be illustrated as in Fig. 1.2.

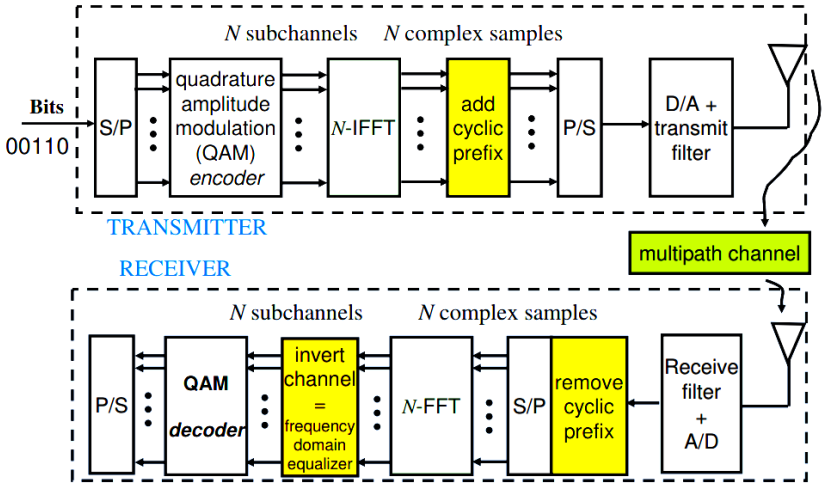

Fig. 1.2 OFDM architecture

OFDM technology is adopted in the *long Term Evolution* (LTE) standard. In LTE the smallest time-frequency unit for transmission is called a resource element. Resource elements are grouped into resource blocks, i.e., group of subcarriers in frequency and one slot in time. Each user can be assigned one or more resource blocks.

1.3 MUTI-INPUT MULTI-OUTPUT (MIMO) SYSTEMS [11]

Multi-input multi-output wireless communication techniques have been known for their ability for high capacity, increased diversity and interference mitigation or suppression. Multi-user MIMO (MU-MIMO) is a technology used to permit different users to access the same band of frequencies at the same time, by multiplexing them in space. There are two scenarios for MU-MIMO transmission, namely, the uplink scenario where multiple users transmit their data to a common base station on the same band of frequencies and the downlink transmission where the base station attempts to send different data to its users over the same band simultaneously.

In MU-MIMO uplink scenario the number of receiving antennas should be greater than or equal to the number of transmitting antennas to enable the receiver to separate the multiple users' transmitted data at the base station so that reliable decoding could be done. There are two types of decoders, linear decoders such as *zero forcing* (ZF) and *minimum mean square error* (MMSE), and nonlinear decoders such as successive interference cancellation with ZF (SIC-ZF), successive interference cancellation with MMSE (SIC-MMSE) and sphere decoders. This requires the base station to estimate the channels of its users, which is done via pilots transmitted by the users.

In MU-MIMO downlink scenario, it is usually preferred to minimize the processing at the users' receivers so the base station has to design the transmitted signals in such a way that each user only receives its intended transmitted data without being interfered with other users' data transmitted from the same base station. Using beamforming techniques at the base station usually does this inter-user interference mitigation. This requires the knowledge of the channels at the base station to its users, which needs some feedback from the users especially when operating in the FDD mode.

Zero forcing beamforming is a simple linear method to deal with the inter-user interference by imposing the constraint that no user suffers from any interference from other user. This is simply done by pre-coding the users' data with the pseudo-inverse of the channel matrix vectors.

Dealing with the inter-user interference by simply inserting the constraint of zero interference terms achieves identical SINR at each user. However, in some networks the

supported services may be heterogeneous with different QoS requirements, hence different required SINR. Many optimal and suboptimal nonlinear beamformers for maximizing the total throughput of users and achieving different QoS constraints were proposed.

MIMO techniques are easily adopted with OFDM systems as the space-time equalizers complexity is avoided because of the flat fading response seen by each subcarrier band [9]. MU-MIMO is a supported transmission mode in the LTE and LTE-Advanced mobile standards. Using MU-MIMO mode in LTE, an OFDM resource block could be shared by multiple users, hence, increasing system capacity. We will exploit this model in Chapter 2 in this thesis.

1.4 COMPRESSIVE SENSING BACKGROUND

1.4.1 ℓ_1 and ℓ_2 regularization[12][13]

- *Definitions:*

- A signal is denoted by a k-sparse signal if it can be represented by at most k non-zero coefficients in a particular domain.

- ℓ_p norm of a vector $\mathbf{v} \in \mathrm{C}^{\mathrm{N}}$ is denoted as $\|\mathbf{v}\|_p = (\sum_{i=1}^{N} |v_i|^p)^{\frac{1}{p}}$

Let $\mathbf{A} \in \mathrm{C}^{\mathrm{M}} \times \mathrm{C}^{\mathrm{N}}$ be a measurement matrix with linearly independent columns, and $\mathbf{v} \in \mathrm{C}^{\mathrm{N}}$ be the unknown k-sparse vector, i.e, it contains at most k non-zero elements, and $\mathbf{y} \in \mathrm{C}^{\mathrm{M}}$ is the vector of observed measurements such that

$$\mathbf{y} = \mathbf{A}\mathbf{v} + \mathbf{n},$$

where $\mathbf{n} \in \mathrm{C}^{\mathrm{N}}$ is an additive noise vector. In case of $M >= N$, this linear model is overdetermined and $\mathbf{v}$ can be determined by solving the least squares problem of minimizing the square error in (1).

$$\min\|\mathbf{y} - \mathbf{A}\mathbf{v}\|_2^2 \quad (1)$$

The closed analytical form for (1) can be written as:

$$\mathbf{v}^* = (\mathbf{A}^H\mathbf{A})^{-1}\mathbf{A}^H\mathbf{y}, (2)$$

which is simply the pseudo-inverse of the measurement matrix $\mathbf{A}$ multiplied by the observation vector $\mathbf{y}$.

Now, consider the case where $M < N$, so we have an underdetermined system of linear equations. Using the above method of minimizing the square error, which is also known as least square regression, results in an overfitting, hence, the vector $\mathbf{v}$ cannot be recovered.

1.4.1.1 ℓ_2 Regularized Least Squares

To avoid over fitting resulting from using the above method, ℓ_2 regularized least squares (LS) also known as Tikhonov regularization can be used. It can be written as

$$\min\|\mathbf{y} - \mathbf{A}\mathbf{v}\|_2^2 + \lambda\|\mathbf{v}\|_2^2, \qquad (3)$$

where $\lambda > 0$ is the regularization parameter. If $\lambda = 1$, we are looking for a solution that minimizes the square error with the smallest energy. ℓ_2 regularized least squares (LS) tends to distribute the energy over the vector solution elements; hence, non sparse vector solution could be obtained. The analytical closed form of (3) can be written as:

$$\mathbf{v}^* = (\mathbf{A}^H\mathbf{A} + \boldsymbol{\lambda}\mathbf{I})^{-1}\mathbf{A}^H\mathbf{y}. \quad (4)$$

In statistics context, this kind of regularization is well known as Ridge regression method where the λ would express some given prior probability distribution for $\mathbf{v}$. In signal processing and communication fields, ℓ_2 regularized LS is known as minimum mean square error MMSE solution when λ equals to the inverse of the average signal to noise interference ratio (SNR).

1.4.1.2 ℓ_1 Regularized Least Squares

Instead of using the second norm, $\|\mathbf{v}\|_2^2$, in (3), ℓ_1-norm is used which is simply the summation of the absolute values of the vector elements as

$$\min\|\mathbf{y} - \mathbf{A}\mathbf{v}\|_2^2 + \lambda\|\mathbf{v}\|_1. \qquad (5)$$

It can be observed that unlike the ℓ_2 regularized LS, ℓ_1 regularization leads to a solution vector that is not linear in $\mathbf{y}$ and it does not have an analytical closed form. Hence numerical methods are used to solve the ℓ_1 regularized LS problem such as interior–point method.

Unlike minimizing $\|\mathbf{v}\|_2^2$, minimizing $\|\mathbf{v}\|_1$tends to give a sparse solution, and by adjusting the regularization parameter λ one can adjust the sparsity level. ℓ_1 regularization is sometimes called basis pursuit denoising; also it is popularized by the name Least Absolute Selection and Shrinkage Operator (LASSO).

1.4.2 **Compressive sensing**

Pioneered by Candes et al.[14], under some constraints on the sensing matrix, a signal can be recovered with fewer measurements or samples than that required by conventional Nyquist sampling approach which states that to be able to reconstruct a signal the sampling rate should be at least twice the bandwidth of that signal. The main idea of compressive sensing is exploiting the sparse structure of a signal. This sparse structure can be found in many natural signals. For example, many natural continuous time signals may have their "information rate" much smaller than that suggested by their bandwidth; also many discrete-time signals may depend on numbers of degrees of freedom which are comparably much smaller than their (finite) length. Compressive Sensing is based on ℓ_1-norm minimization that ensures the sparsity of the recovered signal.

In the aforementioned system model, let $\mathbf{v}$ is the vector signal to be recovered then by numerically solving the problem

$$\min\|\mathbf{y}\|_1 \text{ subject to } \|\mathbf{y}-\mathbf{A}\mathbf{v}\|_2 \leq \epsilon, \qquad (6)$$

recovering the signal $\mathbf{v}$ could be done under certain constraints with certain probability, where ϵ is a function of the noise variance. There are many tools that can solve the above problem that are based on quadratic programming or more generally convex optimization methods; for more information, please refer to [12].

Compressive sensing has been adopted in many works for wideband and multichannel spectrum sensing techniques [15][16].

1.4.3 **Block Sparse Reconstruction**

Some signals exhibits additional structure properties, such that their non-zero elements are arranged in the form of blocks, such signals are denoted as *block sparse* signals. Block sparse structure is naturally found in multichannel signals such as the OFDM signals. By making use of these additional structure properties, a further extension to compressive sensing discussed above is made. It was demonstrated that extending the ℓ_1-norm minimization by making use of block sparse structure that a signal may possess yields a better reconstruction of the signal than treating it as being just conventionally sparse [17][18].

Let $\mathbf{v} \in \mathrm{C}^{\mathrm{N}}$, which is a vector of length N, be divided into k blocks of length d, such that $k = N/d$ is an integer. A vector is referred as k-block spare if it has at most k non-zero blocks. Therefore, the extended problem becomes

$$\min \sum_{i=1}^{k} \left\| \mathbf{v}_{(i-1)d+1:id} \right\|_2 \text{ subject to } \|\mathbf{y} - \mathbf{A}\mathbf{v}\|_2 \leq \epsilon, \qquad (7)$$

where $\mathbf{v}_{(i-1)d+1:id}$ represents the elements of the vector $\mathbf{v}$ whose indices from $(i-1)d+1$ to id. We will make use of this block sparse reconstruction in chapter 2 of this thesis when we try to exploit the spatial spectrum holes since in this case our model will naturally involve block sparse data vectors.

CHAPTER 2
EXPLOITING SPATIAL SPECTRUM HOLES in MULTIUSER MIMO SYSTEMS

In this chapter, a modified spectrum-sensing algorithm for Cognitive Radio is proposed for the detection of spatial spectrum holes. Two scenarios are discussed, namely, the static scenario and the dynamic scenario. In both scenarios, by exploiting a priori information about primary users (PUs) activity, a better sensing for spatial spectrum holes in MU-MIMO can be achieved. This is achieved by utilizing the idea of augmenting zero symbols in the constellation alphabet in conjunction with a Maximum A Posteriori (MAP) detector with relaxed constraints as introduced in [19], which is discussed later in details. This idea is adapted for our problem settings of spatial spectrum holes sensing, and is expanded to deal with the dynamic nature of the PUs in an OFDM by exploiting both the block sparse structure of the OFDM signal being sensed and the knowledge of a priori information about the PUs activity. In the dynamic case, the PUs activity is modeled as a two-state Markov chain. In the following section, we will give a brief introduction of the problem and introduce the spatial spectrum hole concept.

2.1 INTRODUCTION

Cognitive Radio (CR) has emerged as a possible solution for the inefficient utilization of the radio spectrum. The main task of a CR is to sense the spectrum to discover the spectrum holes, upon which the CR can adaptively assign these free spectrum holes to prospective secondary users (SU). As mentioned in the previous chapter, there are many spectrum-sensing techniques that could be used by a cognitive radio to search for an opportunistic transmission for its data without significantly degrading the primary user performance. However, these traditional techniques of spectrum sensing, such as energy detectors, matched-filter detectors, and cyclostationary detectors [20] do not ultimately utilize the available spectrum as there are some opportunities for spectrum sharing they overlook. The fact that in multi-user multi-input multi-output (MU-MIMO) systems the number of antennas at the primary receivers has to be greater than or equal to the number of PUs

transmitters for reliable decoding [20] could be exploited such that secondary users can transmit their data along with the PUs as long as the number of active PUs is less than the number of primary receiving antennas. Consequently, there still exist spatial dimensions that create spatial spectrum holes, which a CR can assign to its users without degrading the performance of the PU network [19]. Hence, a cognitive radio can share with the primary users the degrees of freedom in the PU MIMO system when these degrees of freedom are not fully utilized by the primary users.

Recently, compressive sensing (CS) has been used as an efficient tool, in terms of the required number of measurements to be sensed, to detect or recover sparse signals. In [18], the authors utilized the sparsity of signals along with the finite alphabet constraint to deal with the multiuser detection problem in CDMA system when the activity of users is unknown. They proposed optimal MAP and suboptimal MAP detectors based on the idea of incorporating the users' inactivity by augmenting zero symbol in the alphabet constraint and made use of the compressive sensing techniques for decoding the users' data. Accounting for the block sparsity pattern of OFDM signals, the authors in [20] used CS tools to detect spatial spectrum holes in the uplink of a MU-MIMO OFDM cell. They showed that compressive sensing reconstruction tool performs better than the ordinary MIMO detectors such as Minimum Mean Square Error (MMSE) detector in primary user activity detection. However, only sensing the spatial spectrum holes in a static environment was addressed and a dynamic environment, where users change their states of activity with time, was not considered, which is the more realistic case. Even in the static environment addressed in [20],the probability of primary users' activity was not exploited.

In [21], it was claimed that eigenvalue decomposition of the autocorrelation matrix of the received signal can be used to determine the number of active users, but it needs a huge number of samples for good accuracy of computing the autocorrelation function.

In this chapter, an algorithm for spatial spectrum holes sensing is considered in a dynamic environment exploiting the a priori knowledge of the PUs used constellation and their previously detected activity states. Also, we utilize the idea of augmenting zero symbols in the constellation alphabet introduced in [18]; we adapt this idea for our problem settings of spatial spectrum holes sensing and expand it to deal with the dynamic nature of the PUs in an OFDM system. Simulation results show that the proposed algorithm outperforms the

traditional compressive sensing based method that makes use only of the block sparsity pattern of the signal [20].

The rest of the chapter is organized as follows. The system model and problem formulation will be first presented. Afterwards, a modified sensing strategy is presented for both the static and the dynamic environments. Then simulation results of the proposed modified sensing strategy is presented and compared with the algorithm presented in [20].

2.2 SYSTEM MODEL

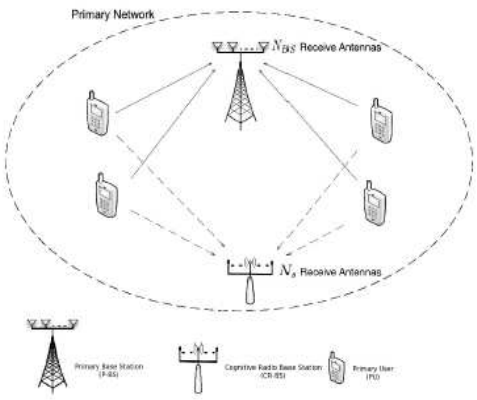

Fig. 2. 1 System Model

An uplink scenario of a single MIMO OFDM cell is considered where a set of single-antenna primary users communicate with a single primary base station (PBS) in a multiuser MIMO settings as shown in Fig. 2.1[1]. Next, the system models for the primary and the secondary networks are described.

2.2.1 Primary User Network

The primary user network has a maximum of N_P active users, sharing the same set of subcarriers, which can simultaneously send their data to their primary base station (PBS) equipped with $N_{BS} \geq N_P$ receiving antennas. The condition $N_{BS} \geq N_P$ guarantees that the PBS will be able to separate the signals from the different users. The number of active PUs, N_a,can be much less than N_{BS} and this allows for some spatial spectrum holes that can be occupied by the SUs since the PBS can separate the interference caused by these SUs on the

[1]MU-MIMO is a supported transmission mode in the LTE and LTE-Advanced mobile standards.

primary network. Each PU sends its OFDM symbol $\mathbf{x}_i$ on L subcarriers with an average transmitted power constraint $\mathrm{E}[\mathbf{x}_i{}^H \mathbf{x}_i] \leq L$.

It is assumed that all PUs symbols $\mathbf{x}_i$'s are of the same constellation for simplicity of presentation but the idea can be easily extended to other scenarios of different PUs' constellations.

2.2.2 Secondary User Network

The secondary user network has a cognitive radio base station (CBS) with N_S antennas in order to sense the instantaneous number of active primary users, hence the free spatial transmission dimensions. These free dimensions can be assigned to the prospective SUs so that they can transmit their data simultaneously with the primary users without highly degrading the performance of the PU network. Our focus in this chapter is on the detection of the number of active primary users sharing the same frequency resource (same set of subcarriers). Note that the number of SUs plus the PUs must not exceed the available transmission dimensions of the primary network (i.e., must be less than NBS for the PBS to be able to separate the signals of the PUs and the interference from the SUs). It is assumed that the CBS has perfect knowledge of the channels between the PUs and N_S base station sensing antennas. It is a reasonable assumption because this channel knowledge can be achieved by channel estimation via the reference signals already being transmitted by the PUs. We assume a slowly fading channel model so that the channel estimates from the previous PU active slots are still valid. The received signal on the k-th subcarrier at the j-th CBS antenna can be written as

$$\mathbf{y}_j(k) = \sum_{i=1}^{N_p} \mathbf{h}_{ji}(k)\, \mathbf{x}_i(k) + \mathbf{n}_j(k)\ , \qquad k = 1, \dots, L, \quad (2.1)$$

where $\mathbf{y}_j$ is an $L \times 1$ vector, $\mathbf{x}_i$ is the transmitted OFDM symbol from the i-th PU, $\mathbf{h}_{ji}(k)$ is the channel gain on the k-th subcarrier between the j-th CBS antenna and the i-th PU and $\mathbf{n}_j$ is a vector of independent identically distributed (i.i.d.) complex Gaussian noise samples received at the j-th CBS antenna with zero mean and covariance matrix $\sigma^2\mathbf{I}$. Collecting the data from the L subcarriers we get

$$\mathbf{y}_{\mathrm{j}} = \sum_{i=1}^{N_p} \mathrm{diag}(\mathbf{h}_{ji})\mathbf{x}_i + \mathbf{n}_j. \quad (2.2)$$

Collecting the received signals from all of the CBS antennas we get

$$\mathbf{y} = \mathbf{H}\mathbf{x} + \mathbf{n}, \quad (2.3)$$

where

$$\mathbf{H} = \begin{bmatrix} \mathrm{D}(\mathbf{h}_{11}) & \mathrm{D}(\mathbf{h}_{12}) \cdots & \mathrm{D}\left(\mathbf{h}_{1N_p}\right) \\ \mathrm{D}(\mathbf{h}_{21}) & \mathrm{D}(\mathbf{h}_{22}) \cdots & \mathrm{D}\left(\mathbf{h}_{2N_p}\right) \\ \vdots & \vdots & \vdots \\ \mathrm{D}(\mathbf{h}_{\mathrm{N_s}1}) & \mathrm{D}(\mathbf{h}_{ji}) \vdots \cdots & \mathrm{D}\left(\mathbf{h}_{N_s N_p}\right) \end{bmatrix}, \quad (2.4)$$

$\mathbf{y} = [\mathbf{y}_1{}^T \mathbf{y}_2{}^T \ldots \mathbf{y}_{N_s}{}^T]$, $\mathbf{x} = [\mathbf{x}_1{}^T \mathbf{x}_2{}^T \ldots \mathbf{x}_{N_P}{}^{\mathrm{T}}]$ and $\mathbf{n} = [\mathbf{n}_1{}^T \mathbf{n}_2{}^T \ldots \mathbf{n}_{\mathrm{N_s}}{}^T]$ are the concatenation of received vectors $\mathbf{y}_{\mathrm{j}}$'s at all CBS antennas, the concatenation of all the PUs symbols vectors $\mathbf{x}_j$'s, and the concatenation of the received noise vectors $\mathbf{n}_j$'s at all CBS antennas, respectively.

2.3 SENSING STRATEGY

2.3.1 Static Environment

Now, our goal is to detect the activity of each PU by sensing the concatenated vector $\mathbf{x}$. Here, we mean by static environment that the probability of activity of the PUs is the available information and no information about the transition probabilities is available.

If the i-th PU is active then its corresponding vector, $\mathbf{x}_i$, can have Q^L possible alphabet vectors, where Q is the constellation size. If the i-th PU is inactive then its corresponding vector, $\mathbf{x}_i$, will be a zero vector.

Assuming that the probability that a PU is active equals p_a then the probability of a zero data vector equals $(1 - p_a)$, while the probability of any possible non-zero vector equals p_a/Q^L(assuming equiprobable data vectors). Then the optimal detector in the Bayes risk

sense is a maximum a posteriori probability (MAP) detector, due to the non-equiprobable nature of the possible data vectors, given by

$$\hat{\mathbf{x}}^{MAP} = \max_{\substack{\mathbf{x}=\left[\mathbf{x}_1{}^T,\ldots,\mathbf{x}_{N_p}{}^T\right] \\ \mathbf{x}_i \in A}} p(\mathbf{y}|\mathbf{x})p(\mathbf{x}), \quad (2.5)$$

where $\mathrm{A} = \{\text{zero vector}, Q^L \text{possible alphapet vectors}\}$.

The prior probability of the concatenated vector $\mathbf{x}$, $p(\mathbf{x})$, can be expressed as

$$p(\mathbf{x}) = \prod_{i=1}^{N_p} \Pr\left(\mathbf{x}_\mathrm{i}\right) = \left(\frac{p_a}{Q^L}\right)^{\frac{\sum_i^{Np}\|\mathbf{x}_i\|_0}{L}} (1-p_a)^{Np-\frac{\sum_i^{Np}\|\mathbf{x}_i\|_0}{L}}, \qquad (2.6)$$

and $p(\mathbf{y}|\mathbf{x})$ is a complex Gaussian distribution with mean $\mathbf{x}$ and covariance matrix $\sigma^2\mathbf{I}$. Then we have

$$\ln p(\mathbf{x}) = \sum_{i=1}^{Np} \frac{\|\mathbf{x}_i\|_0}{L} ln\left(\frac{p_a}{Q^L}\right) + \left(Np - \sum_{i=1}^{Np} \frac{\|\mathbf{x}_i\|_0}{L}\right) ln(1-p_a). \qquad (2.7)$$

The MAP detector reduces to

$$\hat{\mathbf{x}}^{MAP} = \min_{\substack{\mathbf{x}=\left[\mathbf{x_1},\ldots,\mathbf{x}_{N_p}\right] \\ \mathbf{x_i} \in A}} \frac{1}{\sigma^2}\|\mathbf{y}-\mathbf{H}\mathbf{x}\|_2^2 + \lambda \sum_{i=1}^{Np} \|\mathbf{x}_i\|_0, \qquad (2.8)$$

where $= \frac{1}{L}\ln\frac{1-p_a}{p_a/Q^L}$.

Since we have $(Q^L+1)^{N_P}$ possible combinations for the vector $\mathbf{x}$, the MAP detector requires exhaustive search with exponential complexity of order$(Q^L+1)^{N_P}$, which is too large to be implemented in a real time CR since L, the number of subcarriers, is usually large. Therefore, we can relax our problem constraints in (2.8) by ignoring the alphabet constraint and using the mixed ℓ_1/ℓ_2-norm instead of the ℓ_0-norm, leading to a convex optimization problem regularized by λ. Note that λ should be positive to maintain the convexity of the problem [12], and since p_a is small due to the low activity factor (i.e., $p_a \leq 1/2$), λ is always positive.

$$\hat{\mathbf{x}}^{LR} = \min_{\mathbf{x}} \frac{1}{\sigma^2} \|\mathbf{y} - \mathbf{H}\mathbf{x}\|_2^2 + \lambda \sum_{i=1}^{Np} \sqrt{L} \sqrt{\|\mathbf{x}_i\|_2^2}. \qquad (2.9)$$

Note that with the assumption that all the PUs use the same constellation[2] and for the special case that the power on each subcarrier equals one, $\|\mathbf{x}\|_0$ equals $\|\mathbf{x}\|_2$, and the sub-optimality of the detector comes only from the relaxed alphabet constraints.

2.3.2 **Dynamic Environment**

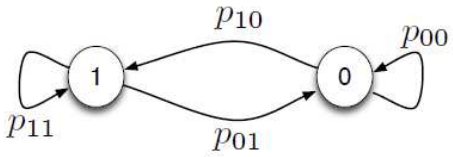

Fig. 2.2 Markov chain model of the PU activity

Now, we consider the dynamic scenario where the activity of each PU can be modeled as a two-state Markov chain [22][23]. The two states are the active state "1" and the inactive state "0" with small transition probabilities, p_{01} and p_{10}, as shown in Fig. 2.2. PUs can assist the CR to obtain these transition probabilities; if this is not the case and there is no cooperation from the PBS these transition probabilities can be estimated as in [24].

We can rewrite (2.9) to adapt it for the dynamic case as

$$\hat{\mathbf{x}}^{LR} = \min_{\mathbf{x}} \frac{1}{\sigma^2} \|\mathbf{y} - \mathbf{H}\mathbf{x}\|_2^2 + \sum_{i=1}^{Np} \lambda_i \sqrt{L} \sqrt{\|\mathbf{x}_i\|_2^2}, \qquad (2.10)$$

where $\lambda_i = \frac{1}{L} \ln \frac{1-P_i}{P_i/Q^L}$.

In the above, the parameter P_i is the probability of the i-th PU to be active. P_i at a certain instant depends on the previous state of the PU, so P_i = Pr[i-th PU active | previous detected activity state of the i-th PU] and it takes the values p_{11} or p_{10} depending on the previous state of the PU.

[2]A constant modulus modulation is assumed.

It is important to note again that the convexity is preserved under positive scaling [12], which is the case in (2.10). To assure that the scaling factors $\{\lambda_i\}$ always takes non-negative values, P_i must be less than or equal to $Q^L/(Q^L+1)$, which is always the case since $Q^L \gg 1$.

2.4 SUMMARY OF THE PROPOSED ALGORITHM

Step (1): Solve the convex problem in (2.9) if not considering the dynamic activity, or the problem in (2.10) if considering the dynamic activity.

Step (2): Zero out all the elements of the estimated vector $\hat{\mathbf{x}}^{LR}$ or $\hat{\mathbf{x}}^{Dyn}$whose values are below the threshold to obtain a vector $\mathbf{x}^{th}$ whose elements are zeroes and ones. This threshold is set to differentiate between the activity states of each subcarrier separately and its value depends on the constellation used.

Step (3): Get ℓ_0-norm of each $\mathbf{x}_i$ and compare it with the threshold $L/2$. If ℓ_0-norm of $\mathbf{x}_i$ for any i is greater than $L/2$ then user i state is declared as active, otherwise it is declared as inactive.

2.5 SIMULATION RESULTS

In this section, we present the simulation results of our modified proposed spatial holes sensing algorithm and compare them to their counterparts.

We simulated an OFDM uplink system with $L = 12$ and $N_P = 8$, i.e., up to 8 different users can share the same 12 subcarriers[3]. The channel between all PUs and all CR antennas are modeled as independent, multipath Rayleigh fading channels with 10 taps and each tap has a variance of $1/10$.

First we considered in Fig. 2.3 the case where the number of active PUs, N_a, changes dynamically according to a Markov model with transition probabilities: $p_{01} = p_{10} = 0.1$and $p_{11} = p_{00} = 0.9$, and with initial probabilities: $p_0 = \Pr[\text{inactive state}] = 0.5$ and $p_1 =$

[3] A resource block in LTE and LTE-Advanced standards is a 12 contiguous subaccariers and it is the smallest unit that can be assigned to a user.

Pr[active state] $= 0.5$. All the transmitted symbols were carved from QPSK constellation. The threshold used equals 0.5.

Fig. 2.3 shows the performance of our proposed detector in equation (2.9) supplying it only with the stationary probability of activity of the PUs, which in our settings equals 0.5. Fig. 2.3 shows also the performance of the proposed detector in equation (2.10) supplying it with transition probabilities. We also show the performance of the CS-based detector of [20] along with the Minimum Mean Square Error MMSE detector.

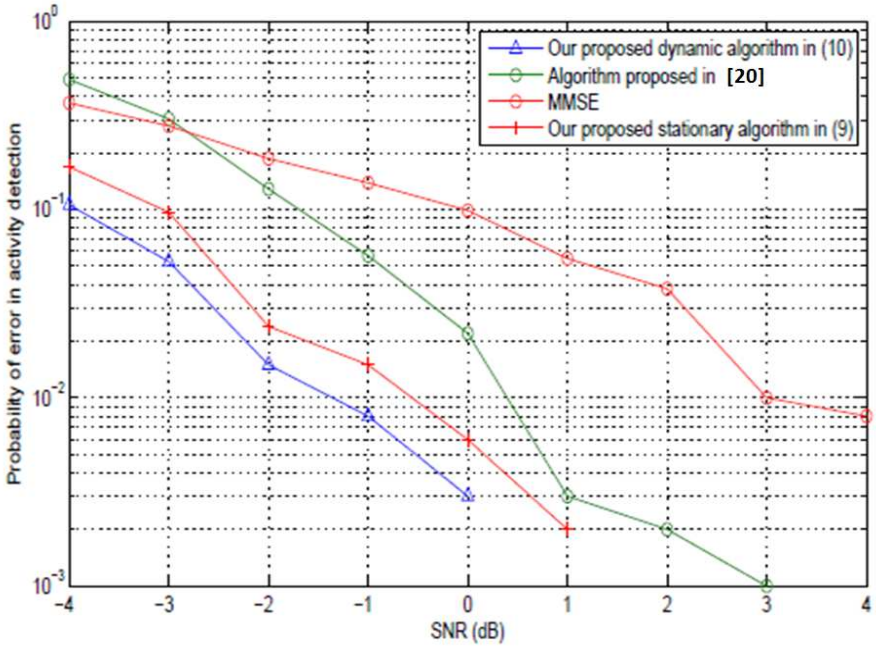

Fig. 2.3 4 QAM

In Fig. 2.4 the same conditions for Fig. 2.3 were considered, but the symbols were carved from 16 QAM constellation and threshold used equals $0.5\sqrt{\frac{2}{10}}$.

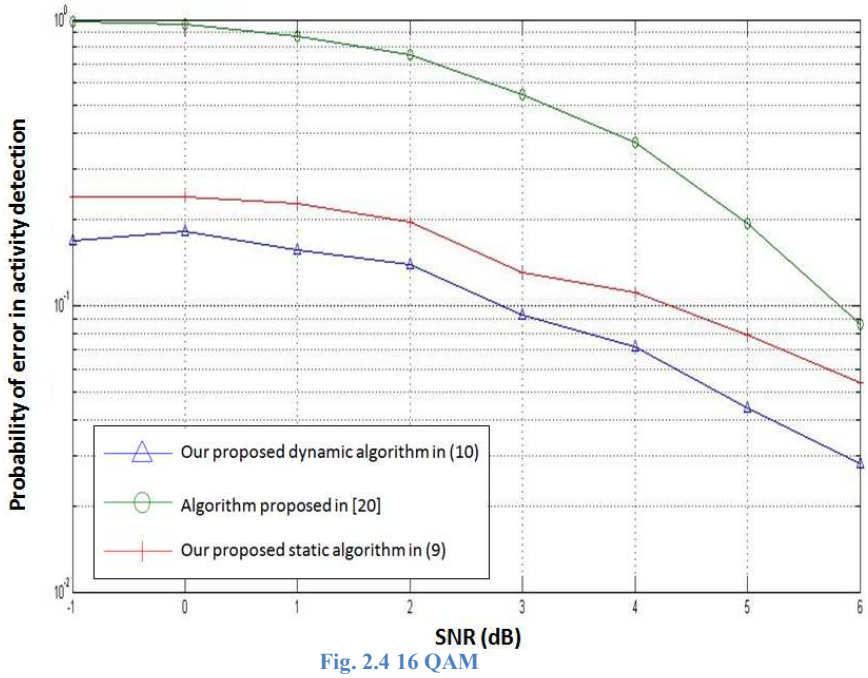

Fig. 2.4 16 QAM

It is clear from the simulation results that our proposed detectors have better performance, as explained before, due to considering both the block sparsity structure of the signal being sensed and the knowledge of the stationary probability of activity in the case of using equation (2.9), and the use of the previously detected states of PUs in the case where the transition probabilities are considered using equation (2.10). It is also clear that the detector that exploits the previously detected states gives the best performance.

2.6 CONCLUSION

In this chapter, an optimal MAP detector and suboptimal MAP-based detectors with relaxed constraints for detecting spatial spectrum holes were proposed. The proposed algorithms make use of the finite alphabet property of transmitted data as well as the a priori PU activity pattern to better detect the number of active primary users. It was shown that better detection performance could be achieved by exploiting the previously detected states of the PUs and the PUs activity patterns. The proposed algorithms outperform the previously proposed algorithms for detecting the spatial spectrum holes.

CHAPTER 3
HIERARCHAL PRIOR ZERO FORCING for COGNITIVE RADIO NETWORKS

In this chapter, cognitive radio relaying in the physical layer is investigated where the cognitive base station (CBS) relays the PU's signal while transmitting its own signals to its secondary uses. A new and simple linear method for beamforming based on zero forcing beamforming adapted for the different levels of priority that users may possess in a cognitive radio network is studied.

3.1 INTRODUCTION

Cognitive radio network (CRN) is a promising solution for alleviating spectrum scarcity problem by utilizing the available spectrum in a more efficient way so that it can meet the dramatic increase in wireless communication demand. Cognitive radio has to protect primary user transmission from the coexisting secondary users. The major task of a CR is how to make its users share the licensed spectrum with the PU without degrading its Quality of Service (QoS). This sharing of the spectrum with the PU is allowed only if the PU will gain help from the SU or at least does not suffer from the SU existence. Cognitive radio can offer assistance to the PU transmission to benefit a higher opportunity for its own transmission; this assistance could be through relaying the PU signal [25].

Many works studied the multi-antenna beamforming [26][27][28][29] in the cognitive radio network considering different levels of channel state information knowledge; however, these works used beamforming to maximize the SUs throughout while limiting the interference to the PU transmission instead of relaying it [30]. In [30], authors proposed a modified zero forcing scheme called *prior zero forcing*(PZF)scheme at the CBS, where the PU is given priority by relaying its signal without considering its interference to the transmissions of the SUs in the system, while the SUs' transmissions are not permitted to cause any interference to the PU transmission. The proposed PZF scheme provides a better effective channel gain for the CBS – PU link compared to the *conventional zero forcing* CZF scheme, thus achieves a lower outage probability for the PU, which is more preferable from the PU point of view. The SU's effective channels achieved by using the PZF scheme were

the same as that using the CZF scheme while the SUs suffered from the PU interference; however, as a result of the PU having better effective channel, the transmitted power needed to ensure its targeted QoS has reduced, so the remaining power at the CBS for the SUs transmissions becomes higher. For studying the complete performance of the PZF scheme and comparing it with the CZF scheme on the SUs, the model of a single SU and PU was studied as a special case in [30]. It was proved that when the target rate of the SU is less than 1 bit/sec/HZ the total required power by the PZF scheme is less than that by the CZF scheme and vice versa [30]. However, in [30], the authors generalized their results by suggesting that there is always a range where the PZF always requires less total power than the CZF, which is not garneted; this will be explained later in the chapter. In the multiple SU case, only the case where all SUs require the same rate was studied, and the case of different rate requirements for each SU was overlooked. Besides the priority of the PU, the cognitive users in a network may have different priorities and each SU may need a different QoS requirement. Another possible scenario for prioritized SUs is when the CR network operator offers different priority levels to its SUs depending on the cost they pay [31].

Nevertheless, most of the research work done in cognitive radio networks treats all SUs equally, while few recent works considered SUs with different priority levels. Moreover, all these works addressed this issue in the multiple access control (MAC) layer only and not in the physical layer, as we will focus in this thesis. In [32][33][34][35], prioritized SUs issue was addressed by developing strategies in the MAC layer for the channel allocation accounting for the different levels of the SUs priorities. For example, in [32] SUs were divided into two levels of priority and "priority-based spectrum handoff" was considered. In [33], a prioritized based allocation scheme was established to consider the different levels of priority for SUs transmissions so that the SUs with higher priority can experience less data transmission delay and channel switches. Power allocation strategy was proposed in [34] for the coexistence of SUs with one of them has higher priority than the others in an uplink scenario. In [35] channels of different holding times were assigned to SUs, such that the SU with the highest priority was allowed to access the channel with the highest holding time.

In this chapter, the different priority levels for SUs are achieved by a newly proposed scheme called *Hierarchal Priority Zero Forcing scheme* HPZF. The proposed HPZF scheme is based on the PZF scheme in [30], and it can be considered as an extension of the later. Unlike other works that consider designing optimal beamforming for relaying the primary

user signal, which use much complex methods such as semi-definite relaxation programming method [36], the target of this chapter is not finding a scheme to design optimal beamforming vectors, but applying the simple linear zero forcing method in a way that can guarantee different levels of protection depending on the hierarchal priority of users in a CRN, which has much less complexity of implementation.

The remainder of the chapter will be organized as follows. First, the system model is presented. Then the different zero forcing schemes pointed out above depending on the level of priority they provide to the users are presented, namely *conventional zero forcing* (CZF), *prior zero forcing* (PZF) and *hierarchal prior zero forcing* (HPZF). Afterwards, the analysis of the HPZF scheme is given. Thereafter, a comparison between the three schemes is conducted. At the end of the chapter simulation results are discussed.

3.2 SYSTEM MODEL

A cognitive radio network (CRN) with one primary user and M secondary users communicating with one cognitive radio base station (CBS) is considered in a certain band of frequencies. The Primary user and all the secondary users are equipped with a single receiving antenna while the CBS is equipped with $L \geq M + 1$ antennas. When the link between PU transmitter and its receiver is good enough the CBS can transmit signals to its secondary users but without causing any interference to the PU using zero forcing beamforming. However, when the PU link is suffering from a deep fading the PU can ask the CBS for assistance, hence the CBS will be in charge of transmitting the PUs signal along with its SUs signals. The CBS firstly decodes the PU signal, and then relay it at the same time it transmits its own signals to its SUs. The priority of the SUs comes after the priority of the PU, which is the basic idea behind a cognitive system. After considering the PU of being the user of the highest priority in the CRN, let the priority of the M SUs is sorted such that the 1st SU has the highest priority among the SUs and the M-th SU has the least priority.

We assume that the CBS uses random Gaussian codebooks; therefore, the transmitted signals can be treated as white Gaussian processes. Let $s_p \sim CN(0, {\sigma_P}^2)$ and $s_i \sim CN(0, {\sigma_i}^2)$ donate the information symbols to be transmitted to the PU and the i-th SU, respectively. Then, the transmitted signal vector by the CBS can be written as:

$$\mathbf{x} = \mathbf{w}_p s_p + \sum_{i=1}^{M} \mathbf{w}_i s_i, \tag{3.1}$$

where $\mathbf{w}_p$and$\mathbf{w}_i$are the beamforming vectors for the PU and the i-th SU, respectively. Then the received signal at the PU can be written as:

$$\mathbf{y}_p = \mathbf{h}_p{}^T \mathbf{w}_p s_p + \mathbf{h}_p{}^T \textstyle\sum_{i=1}^{M} \mathbf{w}_i s_i + \mathbf{n}_p. \tag{3.2}$$

Also, the received signal at the i-th SU can be written as:

$$\mathbf{y}_i = \mathbf{h}_i{}^T \mathbf{w}_i s_i + \mathbf{h}_i{}^T \mathbf{w}_p s_p + \mathbf{h}_i{}^T \textstyle\sum_{\substack{k=1 \\ k \neq i}}^{M} \mathbf{w}_k s_k + \mathbf{n}_i, \tag{3.3}$$

where $\mathbf{h}_p$, $\mathbf{h}_i$, $\mathbf{n}_p$and $\mathbf{n}_i$ are the channel gain between the CBS and PU, the channel gain between the CBS and the i-th SU, noise at PU and thei-th SU, respectively. We assume that the noise variances are equal, $\mathbf{n}_p = \mathbf{n}_i \sim CN(0, {\sigma_n}^2)$.

Then, the received SINR at the PU can be given by:

$$\gamma_{pr} = \frac{\left|\mathbf{h}_p{}^T \mathbf{w}_p\right|^2 \gamma_{pt}}{\sum_{i=1}^{M} \left|\mathbf{h}_p{}^T \mathbf{w}_i\right|^2 \gamma_{it} + 1}, \tag{3.4}$$

while the received SINR at the i-th SU can be given by:

$$\gamma_{ir} = \frac{\left|\mathbf{h}_i{}^T \mathbf{w}_i\right|^2 \gamma_{it}}{\left|\mathbf{h}_i{}^T \mathbf{w}_p\right|^2 \gamma_{pt} + \sum_{\substack{k=1 \\ k \neq i}}^{M} \left|\mathbf{h}_i{}^T \mathbf{w}_k\right|^2 \gamma_{kt} + 1}, \tag{3.5}$$

where $\gamma_{Pt} = \mathrm{E}\left[\left|s_p\right|^2\right]/{\sigma_n}^2$ and $\gamma_{it} = \mathrm{E}[|s_i|^2]/{\sigma_n}^2$. We will denote γ_{Pt} and γ_{it} as the transmit SINR for PU and the transmit SINR for the i-th SU, respectively.

3.3 ZERO FORCING WITH DIFFERENT LEVELS OF PRIORITY

In the following, zero forcing schemes with different levels of priority are illustrated and compared, namely *conventional zero forcing* CZF, *prior zero forcing* PZF and our proposed scheme, *hierarchal prior zero forcing* HPZF. The difference between these

schemes is based on how the beamforming vectors assigned by the CBS to the PU and SUs; this will be illustrated in details in the following subsections.

3.3.1.1 Conventional Zero Forcing [30]

Conventional zero forcing is a simple linear scheme; it is practical for transmitting signals in MU-MIMO systems. It is obtained by simply finding mutual orthogonal beamforming vectors, such that each user beamforming vector is constructed in the null space of the other user's channels. Due to this mutual orthogonality between all the users' beamforming vectors, each user will not experience any interference from the other users in the system.

3.3.1.2 Prior Zero Forcing [30]

Using CZF in our cognitive radio relaying settings, all the users are treated equally. However, this equal treatment strategy violates the priority of the PU, which is a main requirement in a cognitive radio system [31]. Prior zero forcing is a scheme where the PU priority is considered by transmitting the SUs' signals without being allowed to induce any interference on the relayed PU signal, while relaying the PU signal without considering its interference on the SUs.

3.3.1.3 Hierarchal Prior Zero Forcing

In the lately mentioned PZF scheme only the priority of the PU is maintained and all secondary users are treated equally. However, in practical systems SUs may require different priority levels, yet any level of these levels of priority comes after the priority level of the PU. The analysis of this newly proposed HPZF scheme is considered in the next sections along with the comparison results with both PZF and CZF, which will serve as benchmarks.

It is worth mentioning that in this work, the priority levels of the different users are recognized not only from power allocation prospective but also from the signal design.

3.4 HIERARCHAL PRIOR ZERO FORCING ANALYSIS

As illustrated earlier the priority ordering of the users in our cognitive radio network is such that the PU is assigned the highest priority then the priority of the 1st SU comes after

until the M-th SU which is of the least priority. So we aim to find beamforming vectors such that the received signals at each user can be written as:

$$\mathbf{y}_p = \mathbf{h}_p{}^T \mathbf{w}_p s_p + \mathbf{n}_p \tag{3.6}$$

$$\mathbf{y}_i = \mathbf{h}_i{}^T \mathbf{w}_i s_i + \mathbf{h}_i{}^T \mathbf{w}_p s_p + \mathbf{h}_i{}^T \sum_{k=1}^{i-1} \mathbf{w}_k s_k + \mathbf{n}_i \,. \tag{3.7}$$

Therefore, the received SINR at the primary user should be:

$$\gamma_{pr} = \left|\mathbf{h}_p{}^T \mathbf{w}_p\right|^2 \gamma_{pt}, \tag{3.8}$$

while the received SINR at the i-th secondary user should be:

$$\gamma_{ir} = \frac{\left|\mathbf{h}_i{}^T \mathbf{w}_i\right|^2 \gamma_{it}}{\left|\mathbf{h}_i{}^T \mathbf{w}_p\right|^2 \gamma_{pt} + \sum_{k=1}^{i-1} \left|\mathbf{h}_i{}^T \mathbf{w}_k\right|^2 \gamma_{kt} + 1}. \tag{3.9}$$

It is obvious that PU does not suffer from any interference, and each SU only suffers from interference from the users with higher priority than it.

3.4.1 Beamforming Vectors and Effective Channel Gains Calculations

3.4.1.1 CZF Scheme

Adopting CZF to our underlying cognitive radio system, all kinds of users are treated equally. Mathematically speaking, beamforming vectors are chosen such that no user induces interference to anther user; that is

$$\left|\mathbf{h}_k{}^H \mathbf{w}_j\right| \begin{cases} = 0 & \forall\, k \neq j \\ \neq 0 & k = j \end{cases} \tag{3.10}$$

The optimal orthogonal beamforming is simply constructed by finding the pseudo-inverse of the channel matrix. Consequently, the CZF normalized beamforming vectors $\mathbf{w}_p$ and $\mathbf{w}_i$ for the PU and i-th SU respectively can be obtained as follows:

$$\mathbf{w}_p = \mathbf{V}(\mathbf{1}, :)/\|\mathbf{V}(\mathbf{1}, :)\| \,, \tag{3.11}$$

$$\mathbf{w}_i = \mathbf{V}(\mathbf{1} + \mathbf{i}, :)/\|\mathbf{V}(\mathbf{1} + \mathbf{i}, :)\| \tag{3.12}$$

where $\mathbf{V} = \mathbf{H}^{\dagger}$, is the pseudo-inverse of the channel matrix.

Define$\mathbf{H}_c = [\mathbf{h}_1, \mathbf{h}_2, \dots, \mathbf{h}_i, \dots, \mathbf{h}_M]$,and let $\phi_{\mathbf{H}_c}$ represent the null space of $\mathbf{H}_c$, and $\phi_{\mathbf{h}_p}$represent the null space of $\mathbf{h}_p$.

$$\phi_{\mathbf{H}_c} = \mathbf{I} - \mathbf{H}_c \mathbf{H}_c^{\dagger},$$

$$\phi_{\mathbf{h}_p} = \mathbf{I} - \mathbf{h}_p \mathbf{h}_p^{\dagger}.$$

Then, we can write the beamforming vectors as:

$$\mathbf{w}_p{}^* = \frac{\mathbf{h}_p - \underset{\mathbf{H}_i}{\text{Proj}}\, \mathbf{h}_p}{\left\| \mathbf{h}_p - \underset{\mathbf{H}_c}{\text{Proj}}\, \mathbf{h}_p \right\|} = \frac{\phi_{\mathbf{H}_c} \mathbf{h}_p}{\left\| \phi_{\mathbf{H}_c} \mathbf{h}_p \right\|}, \tag{3.13}$$

$$\mathbf{w}_i{}^* = \frac{\mathbf{h}_i - \underset{[\mathbf{h}_p, \mathbf{H}_i]}{\text{Proj}}\, \mathbf{h}_i}{\left\| \mathbf{h}_i - \underset{[\mathbf{h}_p, \mathbf{H}_i]}{\text{Proj}}\, \mathbf{h}_i \right\|}. \tag{3.14}$$

So by going back to equations (3.4) and (3.5) of the received SINR of PU and i-th SU, respectively, we will have:

$$\gamma_{Pr} = \left| \mathbf{h}_p{}^T \mathbf{w}_p \right|^2 \gamma_{pt}, \tag{3.15}$$

$$\gamma_{ir} = \left| \mathbf{h}_i{}^T \mathbf{w}_i \right|^2 \gamma_{it}. \tag{3.16}$$

3.4.1.1.1 Effective Channel Gains

The effective channel gain of the link between the CBS and the PU, (CBS - PU link):

$$G_{pC} = \left| \mathbf{h}_p{}^T \mathbf{w}_p \right|^2 = \left\| \mathbf{h}_p - \underset{\mathbf{H}_c}{\text{Proj}}\, \mathbf{h}_p \right\|^2 = \left\| \phi_{\mathbf{H}_c} \mathbf{h}_p \right\|^2 = \mathbf{h}_p{}^H \phi_{\mathbf{H}_c} \mathbf{h}_p, \tag{3.17}$$

where $\mathbf{H}_c = [\mathbf{h}_1, \dots, \mathbf{h}_i, \dots, \mathbf{h}_M]$, and $\phi_{\mathbf{H}_c}$is the null space of the SUs channels matrix $\mathbf{H}_c$ as described above.

The effective channel gain of the link between the CBS and the i-th SU link, (CBS-ith SU link):

$$G_{iC} = \left\| \mathbf{h}_i{}^T \mathbf{w}_i \right\|^2 = \left\| \mathbf{h}_i - \underset{[\mathbf{h}_p, \mathbf{H}_i]}{\text{Proj}}\, \mathbf{h}_i \right\|^2, \tag{3.18}$$

or equivalently,

$$G_{iC} = \left\| \phi_{\mathbf{H}_i} \mathbf{h}_i - \underset{\phi_{\mathbf{H}_i}\mathbf{h}_p}{\text{Proj}}\, \mathbf{h}_i \right\|^2 = \mathbf{h}_i{}^H \phi_{\mathbf{H}_i} \mathbf{h}_i - \frac{\left| \mathbf{h}_p{}^H \phi_{\mathbf{H}_i} \mathbf{h}_i \right|^2}{\left| \mathbf{h}_p{}^H \phi_{\mathbf{H}_i} \mathbf{h}_p \right|^2}. \tag{3.19}$$

Then,

$$G_{iC} = \mathbf{h}_i{}^H \phi_{\mathbf{H}_i} \mathbf{h}_i \left(1 - \rho_{\mathbf{H}_i}{}^2\right), \tag{3.20}$$

where $\mathbf{H}_i = [\mathbf{h}_1, \dots, \mathbf{h}_{i-1}, \mathbf{h}_{i+1}, \dots, \mathbf{h}_M]$, and $\phi_{\mathbf{H}_i}$is the null space of the SUs channels matrix $\mathbf{H}_i$, and $\rho_{\mathbf{H}_i} = \sqrt{\frac{\left| \mathbf{h}_p{}^H \phi_{\mathbf{H}_i} \mathbf{h}_i \right|^2}{\left| \mathbf{h}_p{}^H \phi_{\mathbf{H}_i} \mathbf{h}_p \right|^2}}$ is the correlation coefficient between $\mathbf{h}_p$ and $\mathbf{h}_i$ in the null space of $\mathbf{H}_i$, i.e,$\phi_{\mathbf{H}_i}$.

3.4.1.2 PZF Scheme

As mentioned earlier, in PZF all SUs signals are not allowed to induce any interference to the PU relayed signal, while the PU does not have such constraint. Consequently, the beamforming vector for the PU signal can be implemented in any signal space [30]. Then the beamforming vector that achieves the largest channel effective gain for the CBS-PU link will be in the same direction of the PU's channel, which resembles the *Maximum ratio transmission* MRT:

$$\mathbf{w}_p{}^* = \frac{\mathbf{h}_p}{\|\mathbf{h}_p\|} \tag{3.21}$$

Clearly we can deduce that PZF beamforming vectors for the secondary users are the same as that for CZF because the orthogonality constraints imposed on the SUs are the same in both cases.

3.4.1.2.1 Effective Channel Gains

The effective channel gain of the CBS-PU link:

$$G_{pP} = \|\mathbf{h}_p\|^2. \tag{3.22}$$

The effective channel gain of the CBS-ith SU link:

$$G_{iP} = \left\|\mathbf{h}_i{}^T \mathbf{w}_i\right\|^2 = \left\|\phi_{\mathbf{H}_i}\mathbf{h}_i - \underset{\phi_{\mathbf{H}_i}\mathbf{h}_p}{\text{Proj}}\,\mathbf{h}_i\right\|^2$$
$$= \mathbf{h}_i{}^H \phi_{\mathbf{H}_i}\mathbf{h}_i - \frac{\left|\mathbf{h}_p{}^H \phi_{\mathbf{H}_i}\mathbf{h}_i\right|^2}{\left|\mathbf{h}_p{}^H \phi_{\mathbf{H}_i}\mathbf{h}_p\right|^2}. \quad (3.23)$$

Then, $$G_{iP} = \mathbf{h}_i{}^H \phi_{\mathbf{H}_i}\mathbf{h}_i(1 - \rho_{\mathbf{H}_i}{}^2). \quad (3.24)$$

Note that the channel effective gains of the secondary users in the PZF case are the same as that in CZF case.

3.4.1.3 HPZF Scheme

To keep the level of interference on each user in the CRN different depending on its priority, the beamforming vectors in the HPZF scheme are:

$$\mathbf{w}_p{}^* = \frac{\mathbf{h}_p}{\left\|\mathbf{h}_p\right\|} \quad (3.25)$$

$$\mathbf{w}_i{}^* = \frac{\mathbf{h}_i - \underset{[\mathbf{h}_p,\mathbf{h}_1,\ldots,\mathbf{h}_{i-1}]}{\text{Proj}}\,\mathbf{h}_i}{\left\|\mathbf{h}_i - \underset{[\mathbf{h}_p,\mathbf{h}_1,\ldots,\mathbf{h}_{i-1}]}{\text{Proj}}\,\mathbf{h}_i\right\|} \quad (3.26)$$

Note that PZF beamforming vector for the least priority secondary user is the same as that using CZF or PZF.

3.4.1.3.1 Effective Channel Gains

The effective channel gain of the CBS-PU link:

$$G_{pH} = \left\|\mathbf{h}_p\right\|^2. \quad (3.27)$$

The effective channel gain of the CBS-ith SU link:

$$G_{iH} = \left\|\mathbf{h}_i{}^T \mathbf{w}_i\right\|^2 = \left\|\mathbf{h}_i - \underset{[\mathbf{h}_p,\mathbf{h}_1,\ldots,\mathbf{h}_{i-1}]}{\text{Proj}}\,\mathbf{h}_i\right\|^2 = \left\|\mathbf{h}_i \phi_{[\mathbf{h}_p,\mathbf{h}_1,\ldots,\mathbf{h}_{i-1}]}\right\|^2, \quad (3.28)$$

where $\phi_{[\mathbf{h}_p,\mathbf{h}_1,\ldots,\mathbf{h}_{i-1}]}$ is the null space of the matrix $[\mathbf{h}_p, \mathbf{h}_1, \ldots, \mathbf{h}_{i-1}]$.

3.4.2 **Required Transmit Power**

3.4.2.1 HPZF Scheme

Now, the total required transmit power in the HPZF case is studied. First, the interference on the users of different priorities is calculated. The notation I_{ki} denotes the interference induced by user k on user i normalized by the noise variance. Let τ_p be the SINR targeted for the PU, while τ_i be the SINR target for the i-th SU.

The PU is the only user that does not suffer from interference from any other user in the system due to its first priority, so $I_{kp} = 0 \; \forall k$. The other users suffer from the users with higher priority than them. So these interferences can be written as follows:

$$I_{ki} = \left|\mathbf{h}_i^{\,T}\mathbf{w}_k\right|^2 \gamma_{ktH} \tag{3.29}$$

Then, the required transmitted power that satisfies the target SINR for the PU can be calculated as:

$$\gamma_{ptH} = \tau_p / G_{pH} \tag{3.30}$$

whereas the required transmitted power that satisfies the target SINR for the i-th SU can be calculated as:

$$\gamma_{itH} = \frac{\tau_i\left(1 + I_{pi} + \sum_{k=1}^{i-1} I_{ki}\right)}{G_{iH}}. \tag{3.31}$$

Note that in this context power refers to the power normalized by the noise variance, which is assumed to be the same for all users.

Then the total required transmit power using HPZF scheme, $\gamma_{total\,H}$, can be written as:

$$\gamma_{total\,H} = \gamma_{ptH} + \sum_{i=1}^{M} \gamma_{itH} = \frac{\tau_p}{G_{pH}} + \sum_{i=1}^{M} \frac{\tau_i\left(1 + I_{pi} + \sum_{k=1}^{i-1} I_{ki}\right)}{G_{iH}}. \tag{3.32}$$

3.5 COMPARING THE DIFFERENT SCHEMES

In this section, the required total power by HPZF scheme is compared with PZF and CZF schemes.

3.5.1 **Comparison between HPZF and PZF**

Now, the total required transmit power for the HPZF and PZF schemes are compared to find a condition at which HPZF can perform better than PZF from the total required transmit power point of view.

The condition for $\gamma_{total\,H} < \gamma_{total\,P}$:

$$\gamma_{ptH} + \sum_{i=1}^{M} \gamma_{itH} < \gamma_{ptP} + \sum_{i=1}^{M} \gamma_{itP}\,, \tag{3.33}$$

$$\frac{\tau_p}{G_{pH}} + \sum_{i=1}^{M} \frac{\tau_i\left(1 + I_{pi} + \sum_{k=1}^{i-1} I_{ki}\right)}{G_{iH}} < \frac{\tau_p}{G_{pC}} + \sum_{i=1}^{M} \frac{\tau_i\left(1 + I_{pi}\right)}{G_{iP}}, \tag{3.34}$$

$$\sum_{i=1}^{M} \frac{\tau_i\left(1 + I_{pi} + \sum_{k=1}^{i-1} I_{ki}\right)}{\left\|\phi_{[\mathbf{h}_p, \mathbf{h}_1, \ldots, \mathbf{h}_{i-1}]}\mathbf{h}_i\right\|^2} < \sum_{i=1}^{M} \frac{\tau_i\left(1 + I_{pi}\right)}{\left\|\phi_{\mathbf{H}_i}\mathbf{h}_i\right\|^2}. \tag{3.35}$$

It could be seen that the i-th SU effective channel gain using HPZF is greater than that using PZF for all users except the SU of the least priority, i.e., $G_{iH} > G_{iP}\ \ \forall\, i \leq (M-1)$, but the i-th SU , except for the 1st SU, suffers more interference in HPZF than that in PZF, depending on its level of priority. Therefore, it is not straightforward to claim which scheme would require less total power for achieving the targeted rates for the different users in the CRN.

3.5.2 **Comparison between HPZF and CZF**

The total required transmit power for the HPZF and CZF cases are compared to find a condition at which HPZF can perform better than CZF from the total required transmit power point of view, the same way used in the above section.

Then the condition for $\gamma_{total\,H} < \gamma_{total\,C}$:

$$\gamma_{ptH} + \sum_{i=1}^{M} \frac{\tau_i\left(1 + I_{pi} + \sum_{k=1}^{i-1} I_{ki}\right)}{G_{iH}} < \gamma_{ptC} + \sum_{i=1}^{M} \frac{\tau_i}{G_{iC}}, \tag{3.36}$$

$$\frac{\tau_p}{G_{pH}} + \sum_{i=1}^{M} \frac{\tau_i\left(1 + I_{pi} + \sum_{k=1}^{i-1} I_{ki}\right)}{\left\|\phi_{[\mathbf{h}_p, \mathbf{h}_1, \ldots, \mathbf{h}_{i-1}]}\mathbf{h}_i\right\|^2} < \frac{\tau_p}{G_{pC}} + \sum_{i=1}^{M} \frac{\tau_i}{\left\|\phi_{\mathbf{H}_i}\mathbf{h}_i\right\|^2}, \tag{3.37}$$

$$\frac{\tau_p}{\left\|\mathbf{h}_p\right\|^2} + \sum_{i=1}^{M} \frac{\tau_i\left(1 + I_{pi} + \sum_{k=1}^{i-1} I_{ki}\right)}{\left\|\phi_{[\mathbf{h}_p, \mathbf{h}_1, \ldots, \mathbf{h}_{i-1}]}\mathbf{h}_i\right\|^2} < \frac{\tau_p}{\left\|\phi_{\mathbf{H}_c}\mathbf{h}_p\right\|^2} + \sum_{i=1}^{M} \frac{\tau_i}{\left\|\phi_{\mathbf{H}_i}\mathbf{h}_i\right\|^2}. \tag{3.38}$$

It could be seen that the i-th SU effective channel gain using HPZF is greater than that using CZF for all users except the SU of the least priority, i.e., $G_{iH} > G_{iP} \ \forall\, i \leq (M-1)$, but in HPZF, the i-th SU suffers from interference induced by the users of higher priority, while in CZF, the i-th SU do not suffer from any interference from any user. Also, it is obvious that the required transmit power for the PU using the HPZF is less than that using the CZF. Therefore, it is not straightforward to claim which scheme would require less total power for achieving the targeted rates for the different users in the CRN.

3.6 SPECIAL CASE

Now, we are going to consider a special case where two SUs, i.e., $M = 2$, of different levels of priority that comes after the priority of the PU are coexisting with the PU.

By using the analysis in the aforementioned sections, the different interference terms can be calculated as:

$$I_{pi} = \left|\mathbf{h}_i{}^H \mathbf{w}_p{}^*\right|^2 \gamma_{ptH} = \frac{\left|\mathbf{h}_i{}^H \mathbf{h}_p\right|^2}{\left\|\mathbf{h}_p\right\|^2} \gamma_{pt} = \frac{\left|\mathbf{h}_i{}^H \mathbf{h}_p\right|^2}{\left\|\mathbf{h}_p\right\|^4} \tau_p, \tag{3.39}$$

$$\begin{aligned} I_{12} &= \left|\mathbf{h}_2{}^T \mathbf{w}_1\right|^2 \gamma_{1tH} \\ &= \frac{\left|\mathbf{h}_2{}^H\left(\mathbf{h}_1 - \mathbf{h}_p \mathbf{h}_p{}^\dagger \mathbf{h}_1\right)\right|^2}{\left\|\mathbf{h}_1 - \mathbf{h}_p \mathbf{h}_p{}^\dagger \mathbf{h}_1\right\|^2} \frac{\tau_1\left(1 + \frac{\left|\mathbf{h}_1{}^H \mathbf{h}_p\right|^2}{\left\|\mathbf{h}_p\right\|^4} \tau_p\right)}{\left\|\mathbf{h}_1 - \mathbf{h}_p \mathbf{h}_p{}^\dagger \mathbf{h}_1\right\|^2} \\ &= \frac{\left|\mathbf{h}_2{}^H\left(\mathbf{h}_1 - \mathbf{h}_p \mathbf{h}_p{}^\dagger \mathbf{h}_1\right)\right|^2}{\left\|\mathbf{h}_1 - \mathbf{h}_p \mathbf{h}_p{}^\dagger \mathbf{h}_1\right\|^4} \tau_1 \left(1 + \frac{\left|\mathbf{h}_1{}^H \mathbf{h}_p\right|^2}{\left\|\mathbf{h}_p\right\|^4} \tau_p\right). \end{aligned} \tag{3.40}$$

Then, the required transmit power for each SU, γ_{itH}, is given by:

$$\gamma_{1tH} = \frac{\tau_1\left(1 + \frac{|\mathbf{h}_1{}^H\mathbf{h}_p|^2}{\|\mathbf{h}_p\|^4}\tau_p\right)}{\left\|\phi_p\mathbf{h}_1\right\|^2}, \tag{3.41}$$

$$\gamma_{2tH} = \frac{\tau_2\left(1 + I_{p2} + I_{12}\right)}{G_{2H}}$$

$$= \frac{\tau_2\left(1 + \frac{|\mathbf{h}_2{}^H\mathbf{h}_p|^2}{\|\mathbf{h}_p\|^4}\tau_p + \frac{|\mathbf{h}_2{}^H(\mathbf{h}_1 - \mathbf{h}_p\mathbf{h}_p{}^\dagger\mathbf{h}_1)|^2}{\|\mathbf{h}_1 - \mathbf{h}_p\mathbf{h}_p{}^\dagger\mathbf{h}_1\|^4}\tau_1\left(1 + \frac{|\mathbf{h}_1{}^H\mathbf{h}_p|^2}{\|\mathbf{h}_p\|^4}\tau_p\right)\right)}{\left\|\mathbf{h}_2 - \underset{[\mathrm{hp\ h1}]}{\mathrm{proj}}\ \mathrm{h2}\right\|^2}$$

$$= \frac{\tau_2\left(1 + \frac{|\mathbf{h}_2{}^H\mathbf{h}_p|^2}{\|\mathbf{h}_p\|^4}\tau_p + \frac{|\mathbf{h}_2{}^H\phi_p\mathbf{h}_1|^2}{\|\phi_p\mathbf{h}_1\|^4}\tau_1\left(1 + \frac{|\mathbf{h}_1{}^H\mathbf{h}_p|^2}{\|\mathbf{h}_p\|^4}\tau_p\right)\right)}{\left\|\phi_p\mathbf{h_2}\right\|^2\left(1 - \frac{|\mathbf{h}_1{}^H\phi_p\mathbf{h}_2|^2}{\|\phi_p\mathbf{h_1}\|^2\|\phi_p\mathbf{h_2}\|^2}\right)}, \tag{3.42}$$

while the required transmit power for the PU, γ_{ptH}:

$$\gamma_{ptH} = \frac{\tau_p}{\left\|\mathbf{h}_p\right\|^2}. \tag{3.43}$$

Then the total required transmitted power using the HPZF scheme, $\gamma_{total\,H}$, can be calculated as:

$$\gamma_{total\,H} = \gamma_{ptH} + \gamma_{1tH} + \gamma_{2tH} \tag{3.44}$$

$$= \frac{\tau_p}{\left\|\mathbf{h}_p\right\|^2} + \frac{\tau_1\left(1 + \frac{|\mathbf{h}_1{}^H\mathbf{h}_p|^2}{\|\mathbf{h}_p\|^4}\tau_p\right)}{\left\|\phi_p\mathbf{h}_1\right\|^2} + \frac{\tau_2\left(1 + \frac{|\mathbf{h}_2{}^H\mathbf{h}_p|^2}{\|\mathbf{h}_p\|^4}\tau_p + \frac{|\mathbf{h}_2{}^H\phi_p\mathbf{h}_1|^2}{\|\phi_p\mathbf{h}_1\|^4}\tau_1\left(1 + \frac{|\mathbf{h}_1{}^H\mathbf{h}_p|^2}{\|\mathbf{h}_p\|^4}\tau_p\right)\right)}{\left\|\phi_p\mathbf{h_2}\right\|^2\left(1 - \frac{|\mathbf{h}_1{}^H\phi_p\mathbf{h}_2|^2}{\|\phi_p\mathbf{h_1}\|^2\|\phi_p\mathbf{h_2}\|^2}\right)},$$

while the total power required using the PZF scheme:

$$\gamma_{total\,P} = \gamma_{ptP} + \gamma_{1tP} + \gamma_{2tP}$$

$$= \frac{\tau_p}{GpP} + \frac{\tau_1\left(1 + \frac{|\mathbf{h}_1{}^H\mathbf{h}_p|^2}{\|\mathbf{h}_p\|^4}\tau_p\right)}{G_{1P}} + \frac{\tau_2\left(1 + \frac{|\mathbf{h}_2{}^H\mathbf{h}_p|^2}{\|\mathbf{h}_p\|^4}\tau_p\right)}{G_{2P}} \tag{3.45}$$

$$= \frac{\tau_p}{\left\|\mathbf{h}_p\right\|^2} + \frac{\tau_1\left(1 + \frac{|\mathbf{h}_1{}^H\mathbf{h}_p|^2}{\|\mathbf{h}_p\|^4}\tau_p\right)}{\left\|\phi_p\mathbf{h_1}\right\|^2\left(1 - \frac{|\mathbf{h}_1{}^H\phi_p\mathbf{h}_2|^2}{\|\phi_p\mathbf{h_1}\|^2\|\phi_p\mathbf{h_2}\|^2}\right)} + \frac{\tau_2\left(1 + \frac{|\mathbf{h}_2{}^H\mathbf{h}_p|^2}{\|\mathbf{h}_p\|^4}\tau_p\right)}{\left\|\phi_p\mathbf{h_2}\right\|^2\left(1 - \frac{|\mathbf{h}_1{}^H\phi_p\mathbf{h}_2|^2}{\|\phi_p\mathbf{h_1}\|^2\|\phi_p\mathbf{h_2}\|^2}\right)}.$$

3.6.1 **Comparison between HPZF and PZF**

In this subsection, the total required transmit powers in HPZF and PZF are compared to find the condition when HPZF is more power efficient than PZF.

$$\begin{gathered}\gamma_{total\,H} < \gamma_{total\,P},\\ \gamma_{ptH} + \gamma_{1tH} + \gamma_{2tH} < \gamma_{ptP} + \gamma_{1tP} + \gamma_{2tP},\\ \frac{\tau_1\left(1+\frac{\|\mathbf{h}_1{}^H\mathbf{h}_p\|^2}{\|\mathbf{h}_p\|^4}\tau_p\right)}{\|\phi_p\mathbf{h}_1\|^2} + \frac{\tau_2\left(1+\frac{\|\mathbf{h}_2{}^H\mathbf{h}_p\|^2}{\|\mathbf{h}_p\|^4}\tau_p + \frac{\|\mathbf{h}_2{}^H\phi_p\mathbf{h}_1\|^2}{\|\phi_p\mathbf{h}_1\|^4}\tau_1\left(1+\frac{\|\mathbf{h}_1{}^H\mathbf{h}_p\|^2}{\|\mathbf{h}_p\|^4}\tau_p\right)\right)}{\|\phi_p\mathbf{h}_2\|^2\left(1-\frac{\|\mathbf{h}_1{}^H\phi_p\mathbf{h}_2\|^2}{\|\phi_p\mathbf{h}_1\|^2\|\phi_p\mathbf{h}_2\|^2}\right)}\\ < \frac{\tau_1\left(1+\frac{\|\mathbf{h}_1{}^H\mathbf{h}_p\|^2}{\|\mathbf{h}_p\|^4}\tau_p\right)}{\|\phi_p\mathbf{h}_1\|^2\left(1-\frac{\|\mathbf{h}_1{}^H\phi_p\mathbf{h}_2\|^2}{\|\phi_p\mathbf{h}_1\|^2\|\phi_p\mathbf{h}_2\|^2}\right)} + \frac{\tau_2\left(1+\frac{\|\mathbf{h}_2{}^H\mathbf{h}_p\|^2}{\|\mathbf{h}_p\|^4}\tau_p\right)}{\|\phi_p\mathbf{h}_2\|^2\left(1-\frac{\|\mathbf{h}_1{}^H\phi_p\mathbf{h}_2\|^2}{\|\phi_p\mathbf{h}_1\|^2\|\phi_p\mathbf{h}_2\|^2}\right)}.\end{gathered} \tag{3.46}$$

After some manipulation, following similar steps to [30], the above inequality could be simplified to

$$\tau_2 < 1. \tag{3.47}$$

Then when $\tau_2 < 1$ or equivalently the target rate of the 2nd SU less than 1 bit/sec/Hz, i.e.,$R_{s2} < 1$ bit/sec/Hz, using HPZF requires less power than that using PZF to satisfy the target rates for all users. Therefore, the selection between the HPZF and PZF schemes only depends on the target rate of the user of the least priority, which in our case is the target rate of the 2nd SU.

To study the gain difference between using the two algorithms, we calculated the following:

$$\gamma_{total\,P} - \gamma_{total\,H} = \tau_1\left(\frac{1}{\|\mathbf{h}_1\|^2(1-\rho_{1p})} + \frac{\rho_{1p}\tau_p}{\|\mathbf{h}_p\|^2(1-\rho_{1p})}\right)\left(1+\frac{\left(1-\tau_2\frac{\|\mathbf{h}_2{}^H\phi_p\mathbf{h}_1\|^2}{\|\phi_p\mathbf{h}_2\|^2\|\phi_p\mathbf{h}_1\|^2}\right)}{\left(1-\frac{\|\mathbf{h}_1{}^H\phi_p\mathbf{h}_2\|^2}{\|\phi_p\mathbf{h}_1\|^2\|\phi_p\mathbf{h}_2\|^2}\right)}\right) \tag{3.48}$$

,

$$\frac{\gamma_{total\ P}-\gamma_{total\ H}}{\gamma_{total\ P}}=\frac{\tau_1\left(\frac{\|\mathbf{h}_p\|^2}{\|\mathbf{h}_1\|^2\left(1-\rho_{1p}\right)}+\frac{\rho_{1p}\tau_p}{\left(1-\rho_{1p}\right)}\right)\left(1+\frac{\left(1-\tau_2\frac{\|\mathbf{h}_2{}^H\phi_p\mathbf{h}_1\|^2}{\|\phi_p\mathbf{h}_2\|^2\|\phi_p\mathbf{h}_1\|^2}\right)}{\left(1-\frac{\|\mathbf{h}_1{}^H\phi_p\mathbf{h}_2\|^2}{\|\phi_p\mathbf{h}_1\|^2\|\phi_p\mathbf{h}_2\|^2}\right)}\right)}{\left(\tau_p+\frac{\tau_1\left(\frac{\|\mathbf{h_p}\|^2}{\|\mathbf{h_1}\|^2}+\rho_{1p}\tau_p\right)}{\left(1-\rho_{1p}\right)\left(1-\frac{\|\mathbf{h}_1{}^H\phi_p\mathbf{h}_2\|^2}{\|\phi_p\mathbf{h_1}\|^2\|\phi_p\mathbf{h_2}\|^2}\right)}+\frac{\tau_2\left(\frac{\|\mathbf{h}_p\|^2}{\|\mathbf{h}_2\|^2}+\rho_{2p}\tau_p\right)}{\left(1-\rho_{2p}\right)\left(1-\frac{\|\mathbf{h}_1{}^H\phi_p\mathbf{h}_2\|^2}{\|\phi_p\mathbf{h_1}\|^2\|\phi_p\mathbf{h_2}\|^2}\right)}\right)}. \tag{3.49}$$

It could be deduced from (3.48) and (3.49) that when the magnitudes of both the channel between the CBS and PU and the channel between the CBS and the 1st SU increase together the gain difference between the HPZF and PZF decreases, and they have approximately the same performance.

3.6.2 **Comparison between HPZF and CZF**

Now, the total required transmit power for the HPZF and CZF schemes are compared to find a condition at which HPZF can perform better than CZF from the total required transmit power point of view. Unfortunately, it is too difficult to get a simple form for determining which scheme performs better. Therefore, we find the condition for this case numerically in the results section. It can be seen that this condition depends on the instantaneous channel values of all the users in the CRN and their target rates.

$$\gamma_{total\ H}<\gamma_{total\ C} \tag{3.50}$$

$$\begin{aligned}\tau_2\left(\frac{1}{\|\mathbf{h}_p\|^2}\rho_{2p}^2\tau_p+\frac{1}{\|\mathbf{h}_1\|^2}\frac{\|\mathbf{h}_2{}^{\mathbf{H}}\phi_p\mathbf{h}_1\|^2}{\|\phi_p\mathbf{h}_2\|^2\|\phi_p\mathbf{h}_1\|^2}\left(\frac{(1-\rho_{2p}^2)}{(1-\rho_{1p}^2)}\right)\tau_1+\frac{1}{\|\mathbf{h}_p\|^2}\frac{\|h_2{}^H\phi_p h_1\|^2}{\|\phi_p\mathbf{h}_2\|^2\|\phi_p\mathbf{h}_1\|^2}\left(\frac{(1-\rho_{2p}^2)}{(1-\rho_{1p}^2)}\right)\rho_{1p}^2\tau_p\tau_1\right)\\ <\frac{\tau_p(1-\rho_{2p}^2)}{\|\mathbf{h}_p\|^2}\left(\frac{1}{(1-\rho_{2p}^2)\left(1-\frac{\|\mathbf{h}_p{}^H\phi_1\mathbf{h}_2\|^2}{\|\phi_1\mathbf{h}_p\|^2\|\phi_1\mathbf{h}_2\|^2}\right)}-1\right)\left(1-\frac{\|\mathbf{h}_1{}^H\phi_p\mathbf{h}_2\|^2}{\|\phi_p\mathbf{h}_1\|^2\|\phi_p\mathbf{h}_2\|^2}\right)\\ -\frac{\tau_1}{(1-\rho_{1p}^2)}\left(\left(\frac{1}{\|\mathbf{h}_1\|^2}+\frac{1}{\|\mathbf{h}_p\|^2}\rho_{1p}^2\tau_p\right)\left(1-\frac{\|h_1{}^H\phi_p h_2\|^2}{\|\phi_p\mathbf{h}_1\|^2\|\phi_p\mathbf{h}_2\|^2}\right)-1\right).\end{aligned}$$

To study the gain difference between the two algorithms, we calculated:

$$\gamma_{total\,C}-\gamma_{total\,H}=\frac{\tau_1\tau_p\rho_{1p}}{\|\mathbf{h}_p\|^2(1-\rho_{1p})}\left(\frac{\left(\frac{\|\mathbf{h}_1{}^H\phi_p\mathbf{h}_2\|^2}{\|\phi_p\mathbf{h}_1\|^2\|\phi_p\mathbf{h}_2\|^2}\right)}{\left(1-\frac{\|\mathbf{h}_1{}^H\phi_p\mathbf{h}_2\|^2}{\|\phi_p\mathbf{h}_1\|^2\|\phi_p\mathbf{h}_2\|^2}\right)}\right)-\frac{\tau_1}{\|\mathbf{h}_1\|^2(1-\rho_{1p}^2)}-\frac{\tau_2\tau_1\left(\frac{\|\mathbf{h}_2{}^H\phi_p\mathbf{h}_1\|^2}{\|\phi_p\mathbf{h}_1\|^2\|\phi_p\mathbf{h}_2\|^2}\frac{(1-\rho_{2p}^2)}{(1-\rho_{1p}^2)}\right)}{\|\mathbf{h}_1\|^2(1-\rho_{2p}^2)\left(1-\frac{\|\mathbf{h}_1{}^H\phi_p\mathbf{h}_2\|^2}{\|\phi_p\mathbf{h}_1\|^2\|\phi_p\mathbf{h}_2\|^2}\right)}$$
$$-\frac{\tau_2\tau_1\tau_p\left(\frac{\|\mathbf{h}_2{}^H\phi_p\mathbf{h}_1\|^2}{\|\phi_p\mathbf{h}_1\|^2\|\phi_p\mathbf{h}_2\|^2}\frac{(1-\rho_{2p}^2)}{(1-\rho_{1p}^2)}\rho_{1p}^2\right)}{\|\mathbf{h}_p\|^2(1-\rho_{2p}^2)\left(1-\frac{\|\mathbf{h}_1{}^H\phi_p\mathbf{h}_2\|^2}{\|\phi_p\mathbf{h}_1\|^2\|\phi_p\mathbf{h}_2\|^2}\right)},$$

(3.51)

$$\frac{\gamma_{total\,H}-\gamma_{total\,C}}{\gamma_C}=\frac{\frac{\tau_p}{\|\mathbf{h_p}\|^2}\left(1-\frac{1}{(1-\rho_{1p})\left(1-\frac{\rho_{2p}}{1}\right)}\right)+\tau_1\left(\frac{1}{\|\mathbf{h}_1\|^2(1-\rho_{1p})}+\frac{1}{(1-\rho_{1p})\|\mathbf{h_p}\|^2}\rho_{1p}\tau_p-\frac{1}{\|\mathbf{h}_1\|^2(1-\rho_{1p})\left(1-\frac{\rho_{12}}{p}\right)}\right)}{\frac{\tau_p}{\|\phi_1\mathbf{h_p}\|^2\left(1-\rho_{\frac{2p}{1}}\right)}+\frac{\tau_1}{\|\phi_p\mathbf{h_1}\|^2\left(1-\frac{\rho_{12}}{p}\right)}+\frac{\tau_2}{\|\phi_p\mathbf{h_2}\|^2\left(1-\frac{\rho_{12}}{p}\right)}}+$$
$$\frac{\frac{\tau_2\left(\|\mathbf{h}_p\|^2\frac{\rho_{2p}}{(1-\rho_{2p})}\tau_p+\tau_1\left(\frac{\rho_{12/p}}{\|\mathbf{h}_1\|^2(1-\rho_{1p})}+\frac{1}{\|\mathbf{h_2}\|^2\|\mathbf{h_p}\|^2}\frac{\rho_{12/p}\ \rho_{1p}}{(1-\rho_{1p})(1-\rho_{2p})}\tau_p\right)\right)}{(1-\rho_{12/p})}}{\frac{\tau_p}{\|\phi_1\mathbf{h_p}\|^2(1-\rho_{2p/1})}+\frac{\tau_1}{\|\phi_p\mathbf{h_1}\|^2(1-\rho_{12/p})}+\frac{\tau_2}{\|\phi_p\mathbf{h_2}\|^2(1-\rho_{12/p})}},$$

(3.52)

where $\rho_{2p/1}=\sqrt{\frac{\|\mathbf{h}_2{}^H\phi_1\mathbf{h}_p\|^2}{\|\phi_1\mathbf{h_2}\|^2\|\phi_1\mathbf{h_p}\|^2}}$, $\rho_{12/p}=\sqrt{\frac{\|\mathbf{h}_1{}^H\phi_p\mathbf{h}_2\|^2}{\|\phi_p\mathbf{h_1}\|^2\|\phi_p\mathbf{h_2}\|^2}}$.

From the previous equation, it could be seen with the increase of the magnitude of both the PU and 1st SU channels with respect to the magnitude of the 2nd SU channel, the performance gain decreases between the HPZF and CZF schemes.

3.6.3 **Comparison between PZF and CZF [30]**

Comparing the total required transmitted power in PZF and CZF to find the condition where PZF more power efficient than CZF, we get

$$\tau_2<\frac{(1-\rho_{2p}{}^2)}{\rho_{2p}{}^2}\left(\left(1-\frac{\|\mathbf{h}_1{}^H\phi_p\mathbf{h}_2\|^2}{\|\phi_p\mathbf{h_1}\|^2\|\phi_p\mathbf{h_2}\|^2}\right)\left(\frac{1}{(1-\rho_{1p}{}^2)\left(1-\frac{\|\mathbf{h}_p{}^H\phi_1\mathbf{h}_2\|^2}{\|\phi_1\mathbf{h_p}\|^2\|\phi_1\mathbf{h_2}\|^2}\right)}-1\right)-\tau_1\frac{\|\mathbf{h}_1\|^2}{\|\mathbf{h_p}\|^2}\frac{\rho_{1p}{}^2}{(1-\rho_{1p}{}^2)}\right),$$

(3.53)

One can find that depending on the channels magnitudes ratio there are cases where CZF always performs better than the PZF.

It is obvious that PZF outperforms CZF when the target SINR of the 2nd SU, τ_2, is less than a certain value that is a function of the PU and 1st SU channels magnitudes.

To study the power gain difference between using the two algorithms, we calculated

$$\gamma_{total\,C} - \gamma_{total\,P} = \frac{\tau_p}{\|\mathbf{h}_p\|^2}\left(\frac{(1-\tau_1\rho_{1p})}{(1-\rho_{1p})\left(1-\frac{\|\mathbf{h_1}^H\phi_p\mathbf{h_2}\|^2}{\|\phi_p\mathbf{h_1}\|^2\|\phi_p\mathbf{h_2}\|^2}\right)} - \frac{\tau_2\rho_{2p}}{(1-\rho_{2p})\left(1-\frac{\|\mathbf{h_1}^H\phi_p\mathbf{h_2}\|^2}{\|\phi_p\mathbf{h_1}\|^2\|\phi_p\mathbf{h_2}\|^2}\right)} - 1\right), \tag{3.54}$$

$$\frac{\gamma_{total\,C} - \gamma_{total\,P}}{\gamma_{total\,C}} = \frac{\frac{\tau_p}{\|\mathbf{h}_p\|^2}\left(\frac{(1-\tau_1\rho_{1p})}{(1-\rho_{1p})\left(1-\frac{\|\mathbf{h_1}^H\phi_p\mathbf{h_2}\|^2}{\|\phi_p\mathbf{h_1}\|^2\|\phi_p\mathbf{h_2}\|^2}\right)} - \frac{\tau_2\rho_{2p}}{(1-\rho_{2p})\left(1-\frac{\|\mathbf{h_1}^H\phi_p\mathbf{h_2}\|^2}{\|\phi_p\mathbf{h_1}\|^2\|\phi_p\mathbf{h_2}\|^2}\right)} - 1\right)}{\frac{\tau_p}{\|\mathbf{h_p}\|^2(1-\rho_{1p})\left(1-\frac{\|\mathbf{h_p}^H\phi_1\mathbf{h_2}\|^2}{\|\phi_1\mathbf{h_p}\|^2\|\phi_1\mathbf{h_2}\|^2}\right)} + \frac{\tau_1}{\|\mathbf{h_1}\|^2(1-\rho_{1p})\left(1-\frac{\|\mathbf{h_1}^H\phi_p\mathbf{h_2}\|^2}{\|\phi_p\mathbf{h_1}\|^2\|\phi_p\mathbf{h_2}\|^2}\right)} + \frac{\tau_2}{\|\mathbf{h_2}\|^2(1-\rho_{2p})\left(1-\frac{\|\mathbf{h_1}^H\phi_p\mathbf{h_2}\|^2}{\|\phi_p\mathbf{h_1}\|^2\|\phi_p\mathbf{h_2}\|^2}\right)}}. \tag{3.55}$$

From (3.53) and (3.54), we can see that by increasing the magnitude of $\mathbf{h}_\mathrm{p}$ the range where PZF outperforms CZF increases. On the other hand, the gain difference is decreased until it becomes insignificant and the two algorithms, PZF and CZF, give almost the same performance. This will become more obvious in the simulation results Section.

3.7 SIMULATION RESULTS AND DISCUSSION

In this section the simulation results for the performance of the CZF, PZF and HPZF schemes given to confirm our previous analysis and to observe the factors that could affect their performance.

3.7.1 Total Required Power

The parameters for the following simulations are as follows. CBS was equipped with *L* antennas, and all the links between the CBS and the SUs and the link between CBS and the PU were assumed to experience i.i.d. Rayleigh fading with a variance of 1.

The next figures show the total required transmitted power against the targeted rate for the least priority SU.

Fig. 3.1 shows the results for the case of M=2, i.e., two SUs were active, where the targeted rates for the PU and all the SUs were equal, (i.e.,$R_p = R_{s1} = R_{s2}$).

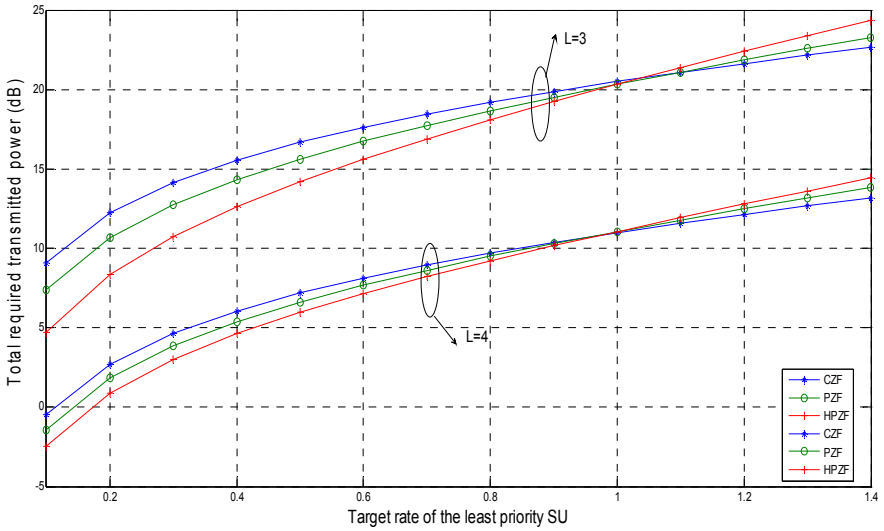

Fig. 3.1 Comparison of the required transmit power: M=2, L=3, 4,$R_p = R_{s1} = R_{s2}$.

In the following figures different targeted rates for PU and the SUs were considered. In Fig. 3.2 the target rate for the PU and 1st SU were set to be 1 bit/sec/HZ.

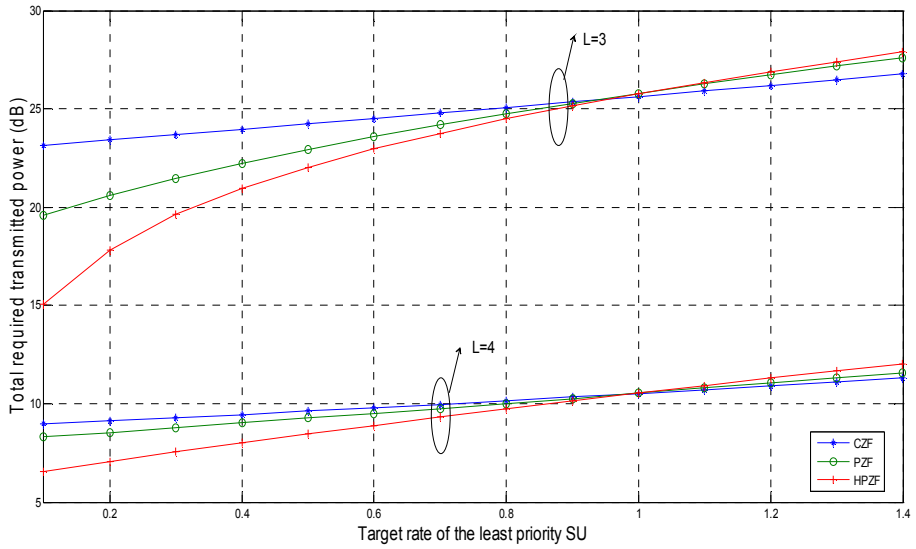

Fig. 3.2 Comparison of the required transmit power: M=2, L=3, 4, $R_p = 1$, $R_{s1} = R_{s2}$.

It could be seen that when the target rate of the SU of the least priority is less than 1, i.e., $R_{s2} < 1$, HPZF requires less total power than the PZF, which is consistent with our analytical analysis.

Also it could be deduced from the above figures that with increasing the number of transmitting antennas at the CBS, L, the differences in performance gains decrease.

In Fig. 3.3 the targeted rates for the PU and 1st SU were set to 2 bits/sec/Hz and 1.5 bits/sec/HZ, respectively, with L=5. It can be seen that HPZF outperforms the CZF as long as the target rate for the 2ndSU is less than about 0.73 bits/sec/Hz, while HPZF outperforms the PZF as long as the target rate for the 2ndSU is less than 1 bits/sec/Hz. Also, the figure shows that the PZF performs better than the CZF only in a small range, where the target rate for the 2nd SU less than about 0.2.

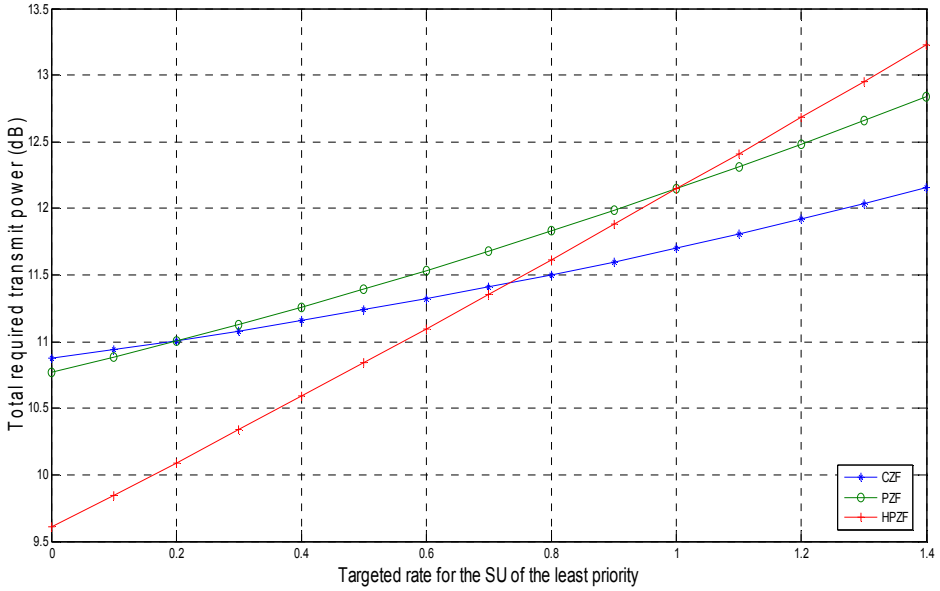

Fig. 3.3 Comparison of the required transmit power: M=2, L=5, $R_p = 2$, $R_{s1} = 1.5$.

In Fig. 3. 4, the targeted rates for the PU and 1st SU were set to 1.5 bits/sec/HZ and 2 bits/sec/Hz, respectively, with $L = 5$. HPZF outperforms the PZF as long as the target rate for the 2nd SU is less than 1 bit/sec/Hz. It can be seen that the CZF always outperforms the PZF, while the HPZF outperforms the CZF for the range where the target rate for the 2nd SU less than 0.6 approximate. Fig. 3.5 shows the results for different set of parameters.

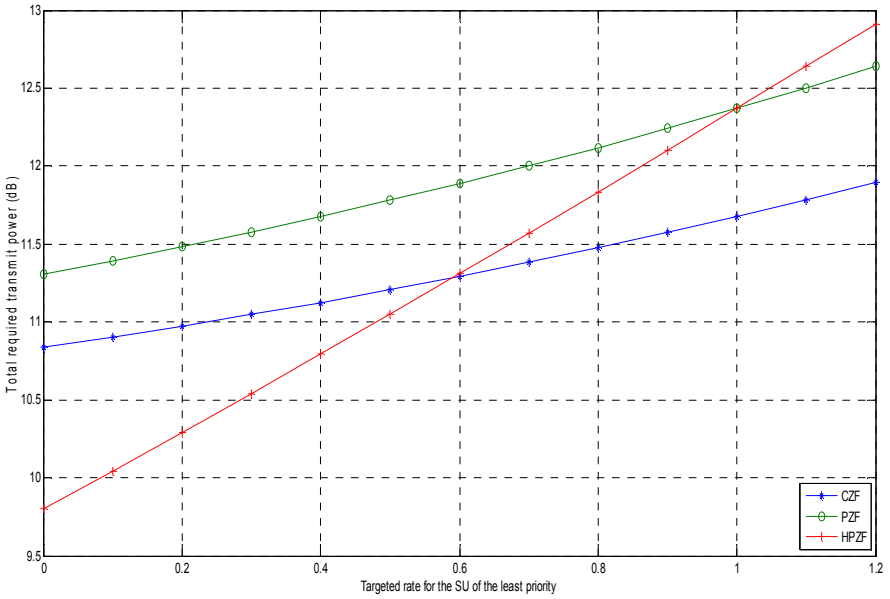

Fig. 3. 4 Comparison of the required transmit power: M=2, L=5, $R_p = 1.5$, $R_{s1} = 2$.

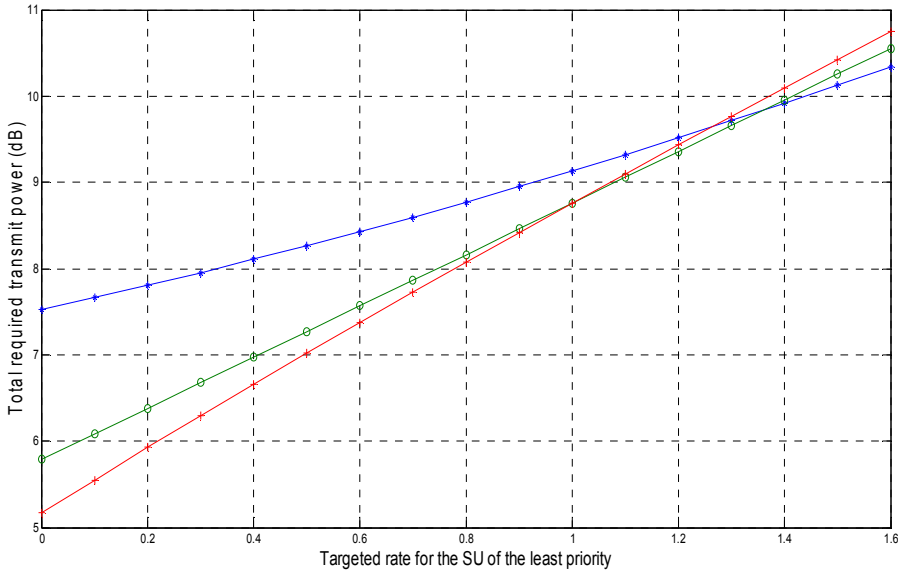

Fig. 3.5 Comparison of the required transmit power: M=2, L=5, $R_p = 1.5$, $R_{s1} = 0.5$.

3.7.1.1 Channel Effects

Now, the effects of the channels variances between the CBS and the different users on the performance of the three schemes from the total required transmit power point of view were examined and the results are illustrated in the following simulation results.

First, the channel variance between the CBS and PU was varied with respect to the other channel variances to study its effect on the performance gain difference between the three schemes, while both the variances for the channel between the CBS and the 1st SU, and the channel between CBS and 2nd SUs were remained to be 1. The PU channel variance was set to be 1, 2 and 4, respectively. In Fig. 3.6 the targeted rates for the SUs were set to be equal and the target rate for the PU was set to 1 bits/sec/Hz, with $L = 3$.

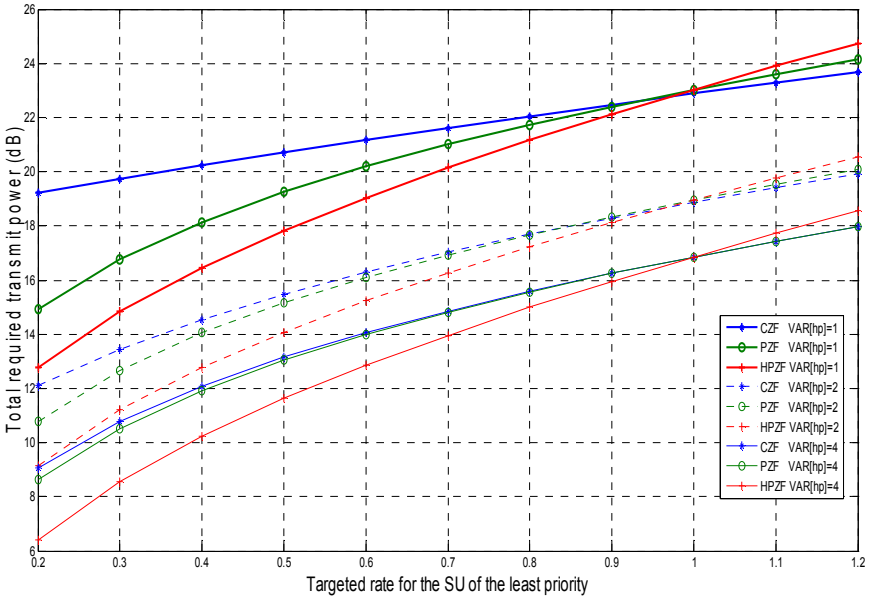

Fig. 3.6 CBS-PU channel variance effect, M=2,L=3.

From Fig. 3.6, when the variance of the channel between the CBS and PU is high with respect to the other channels variances, CZF and PZF perform approximately the same. This result could be seen intuitively since when the magnitude of the channel between the CBS and PU is high this means that the link between the CBS and the PU is good enough to guarantee the targeted rate for the PU with low transmitted power; so the required power for the PU data transmission will be small using both schemes. Also this small power assigned to the PU transmission produces small interference on the SUs, hence, small power is required to compensate for this interference.

In the following the effect of the channel variance between the CBS and 1st SU effect on the performance gain difference between the 3 schemes is illustrated. In Fig. 3.7 the variance of the channel between the CBS and the 1st SU was varied, while the other channel variances are fixed to be 1. The 1st SU channel variance was set to be 1, 2 and 4, respectively.

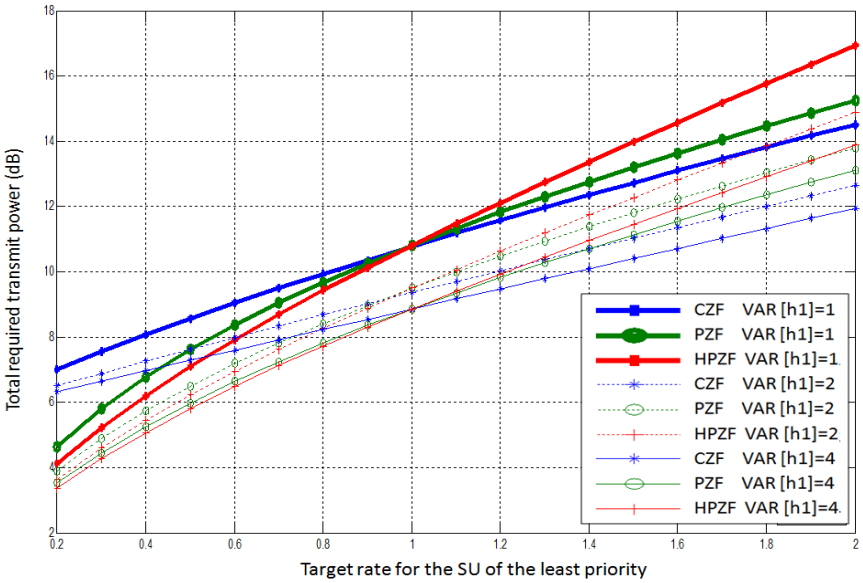

Fig. 3.7 CBS-1st SU channel variance effect, M=2, L=3.

It can be seen that when the ratio between the variances of the PU channel and 2nd SU channel is equal to 1, there is still a significant performance gain difference between the three schemes, especially for the range where $R_{s1} > 1$, even with increasing the 1st SU channel variance with respect to the other channel variances.

In Fig. 3.8, both the PU and 1st SU were set to be 1, 2 and 4, respectively, while the 2nd SU channel variance remained to be 1.

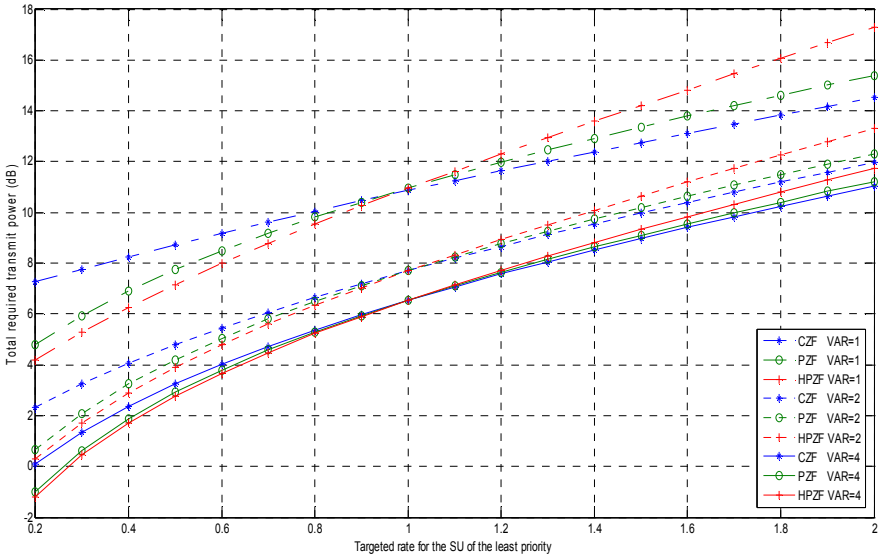

Fig. 3.8 CBS- Varying both CBS-1st SU and CBS-PU channels variances, M=2, L=3.

It could be seen from Fig. 3.8 that when the variances of both the PU channel and the 1st SU channel increase together with respect to the 2nd SU channel variance, the HPZF performance get closer to the PZF performance and consequently get closer to the CZF performance for all values R_{s2}, i.e., the rate of the 2nd SU with the least priority.

Fig. 3.9 shows the total required transmit power against the target rates of both the PU, R_p, and the 1st SU, R_{s1}, for the case where the target rate of the 2nd SU equals 1 bit/sec/Hz, which is the critical point between the HPZF and PZF schemes. It could be observed from the 3D figure that as long as the target rate for the 1st SU is less than 1 bit/sec/Hz,the HPZF needs less total transmit power for achieving the target rates than that required by the CZF scheme, and of course the PZF scheme[4].

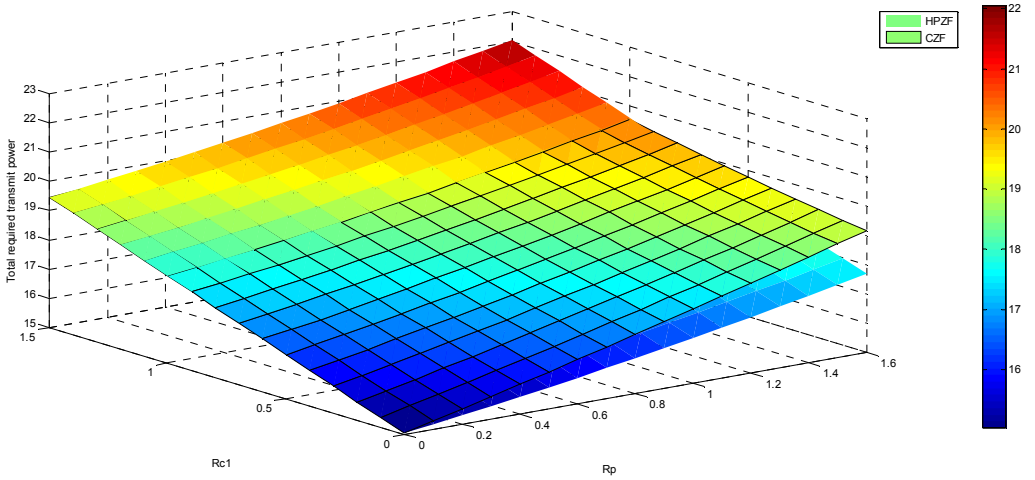

Fig. 3.9 Total required transmit power against both R_p and R_{s1}, L=3, M=2, $R_{s2} = 1$.

3.7.2 Outage Performance

In this subsection, the results simulated for studying the outage performance of the CZF, PZF and HPZF schemes for the different users in the CRN are shown. We first considered the case where the CBS supports two SUs, $M = 2$, and then three SUs, $M = 3$, with different levels of priority.

[4] Since the simulation is done at the critical point $R_{s2} = 1$.

The parameters for the following simulations are as follows. CBS was equipped with $L = 4$ antennas, and all the links between the CBS and the SUs and the link between CBS and the PU were assumed to experience i.i.d. Rayleigh fading with a variance of 1.

- ***Case M=2***

  - **Outage Performance of the PU**

In Fig. 3.10, we compare the CZF, PZF and HPZF with respect to the outage performance of the PU. Two cases were considered for the PU target rate, which were set to be 1 bit/sec/Hz and 3 bit/sec/Hz, respectively. As observed, the HPZF and CZF schemes have the same outage probability since both of them treat the PU with the same priority. Also, the outage performance for the PU using HPZF or PZF always outperforms that using the CZF scheme. It should be mentioned that only the outage performance of the PU using the HPZF or PZF schemes is not affected by the number of SUs supported by CBS or their target rates since the PU in the HPZF or PZF schemes has the first priority in both power allocation and signal design.

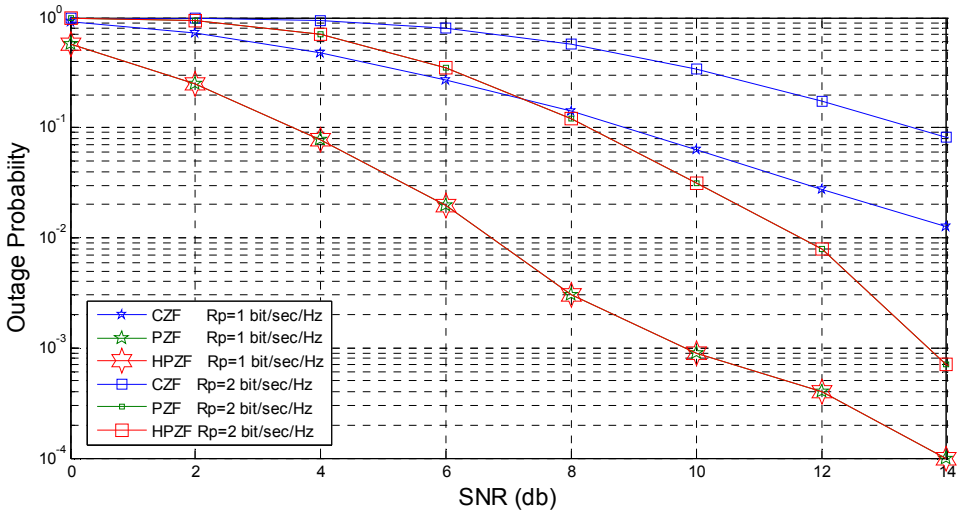

Fig. 3.10 Outage performance of the PU, M=2, L=4.

  - **Outage Performance of the SUs**

In Fig. 3.11,we considered different target rates for the 1st SU, which were set to be 0.5, 1 and 1.5 bit/sec/Hz, respectively, while the other users were set to 1 bit/sec/Hz.It is observed that the outage performance for the 1st SU using the HPZF scheme outperforms both the PZF and CZF schemes.

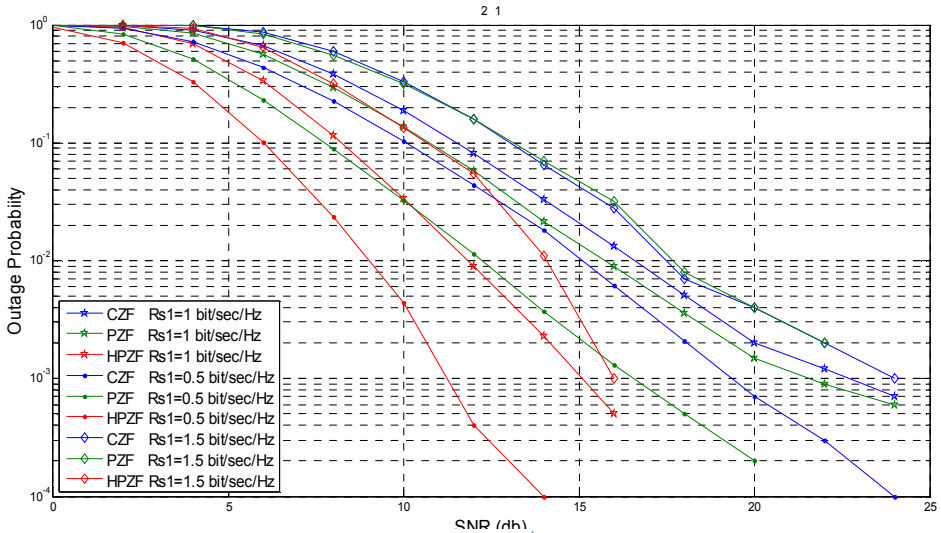

Fig. 3.11 Outage performance of the 1st SU, M=2, L=4.

In Fig. 3.12, we also considered different target rates for the 2nd SU, which were set to be 0.5, 1 and 1.5 bit/sec/Hz, respectively, while the other users were set to 1 bit/sec/Hz. It is observed that for the case when the target rate for the 2nd SU equals 1bit/sec/Hz, the outage performances using the HPZF and the PZF schemes are typically the same, and CZF scheme performance is approximately the same as HPZF and PZF. In the case where the target rate for the 2nd SU equals 0.5 the HPZF gives better outage performance than both the PZF and CZF, while the CZF has the worst outage performance for the 2nd SU. However, the opposite happens when the target rate for the 2nd SU equals 1.5.

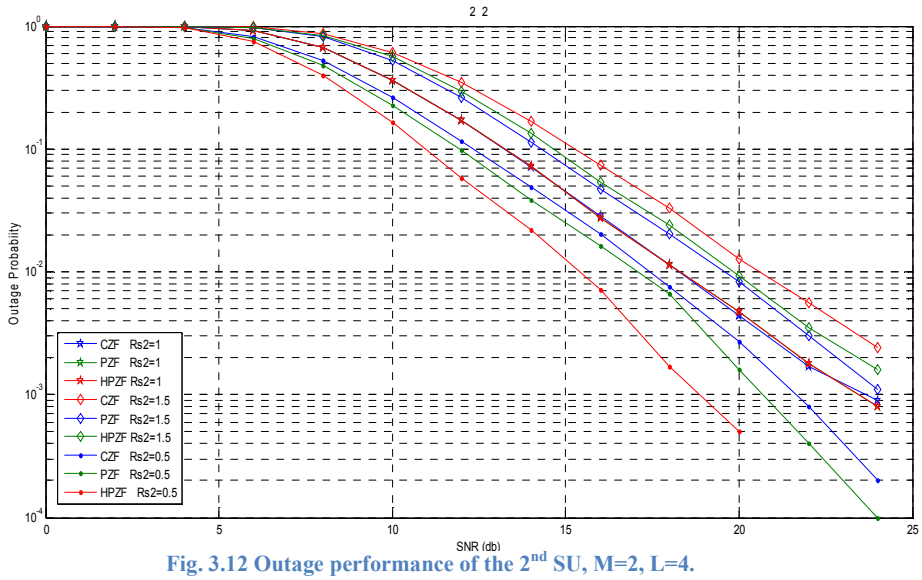

Fig. 3.12 Outage performance of the 2nd SU, M=2, L=4.

- ***Case M=3***

  - **Outage Performance of the PU**

As mentioned earlier, the outage performance of the PU using HPZF is not affected by the number of SUs supported by CBS, since the PU has the 1st priority in both power allocation and beamforming design.

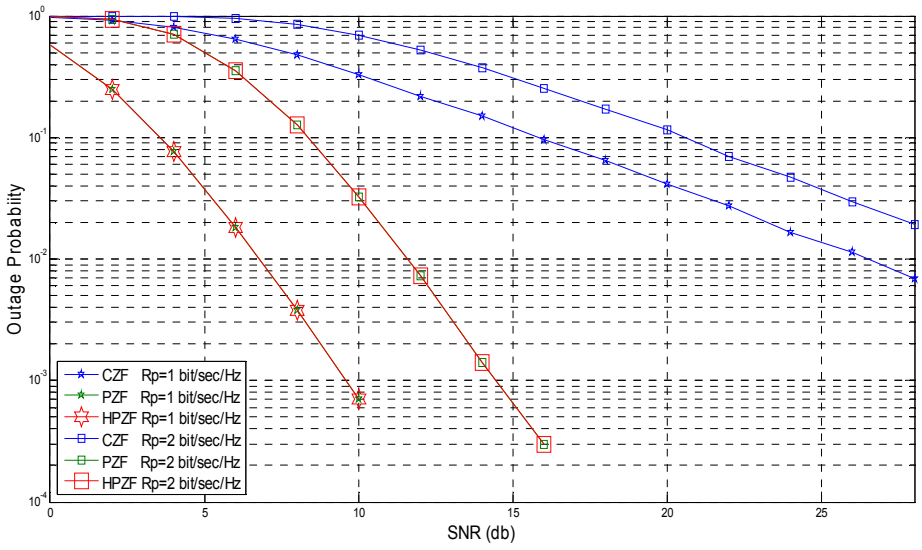

Fig. 3.13 Outage performance of the PU, M=3, L=4.

- **Outage Performance of the SUs**

In this subsection, the CZF, PZF and HPZF are compared with respect to the outage performance of the SUs. The target rate for the PU was set to be 1 bit/sec/Hz.

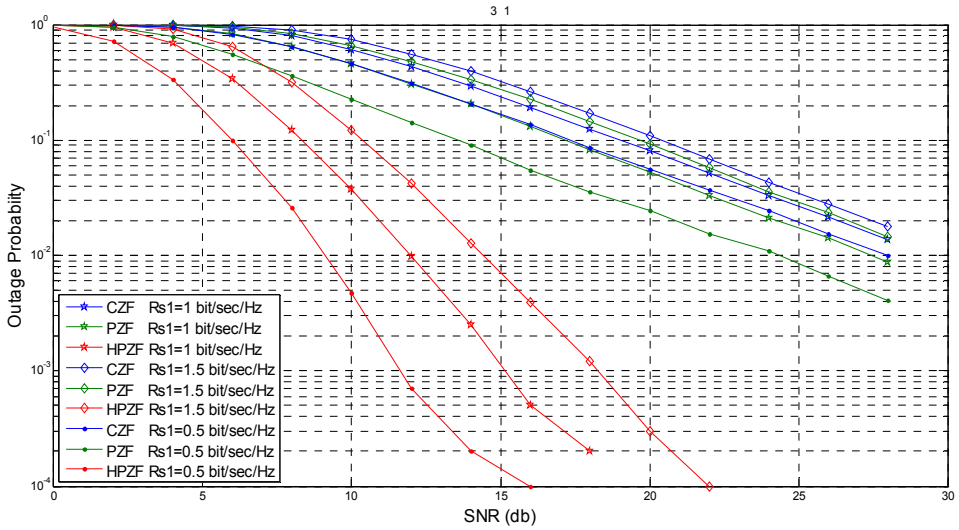

Fig. 3.14 Outage performance of the 1st SU, M=3, L=4.

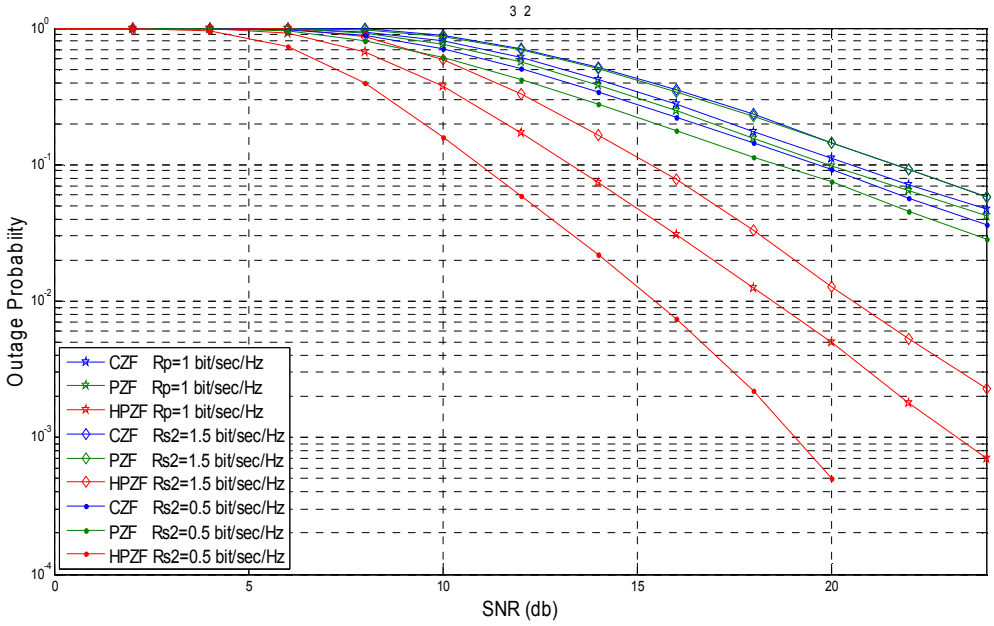

Fig. 3.15 Outage performance of the 2nd SU, M=2, L=4.

Since the HPZF preserves the priority of each user in the CRN, the HPZF outage performance for both the 1st and 2nd SUs will be same, while that for the PZF and CZF will deteriorate with introducing new SUs. Therefore, the outage

performance of the 1st and the 2nd SUs using the HPZF scheme outperforms that using CZF and PZF schemes, as it is seen from Fig. 3.14 and Fig. 3.15.

Now, we show the results regarding the least priority SU, i.e. the 3rd SU. In Fig. 3.16, different target rates for the 3rd SU, the user of the least priority, were considered, which were set to be 0.5, 1 and 1.5 bit/sec/Hz, respectively. It is observed that for the case when the target rate for the 3rd SU equals 1bit/sec/Hz, the outage performances using the three schemes are almost the same. In the case where the target rate for the 3nd SU equals 0.5 the HPZF gives better outage performance than both the PZF and CZF, while the CZF has the worst outage performance for the 3nd SU. However, the opposite happens when the target rate for the 2nd SU equals 0.5.

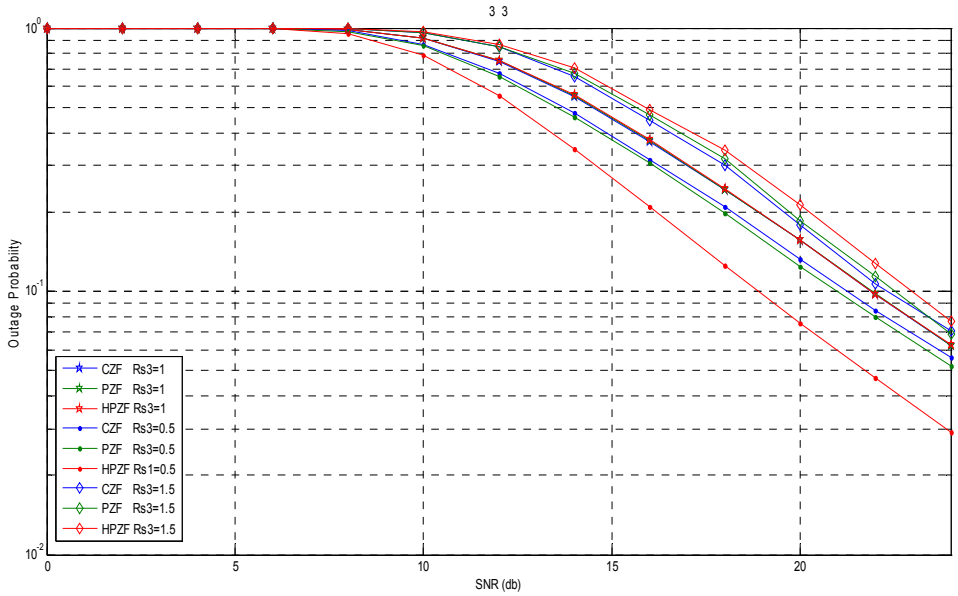

Fig. 3.16 Outage performance of the 3nd SU, M=3, L=4.

It is worth mentioning that in case new SUs demand services from the CBS, HPZF preserves the priority for each user whatever the number of extra new users entering to the network.

Fig. 3.17 shows the case of M=4 SUs having the same target rates, while the PU target rate equals 1.

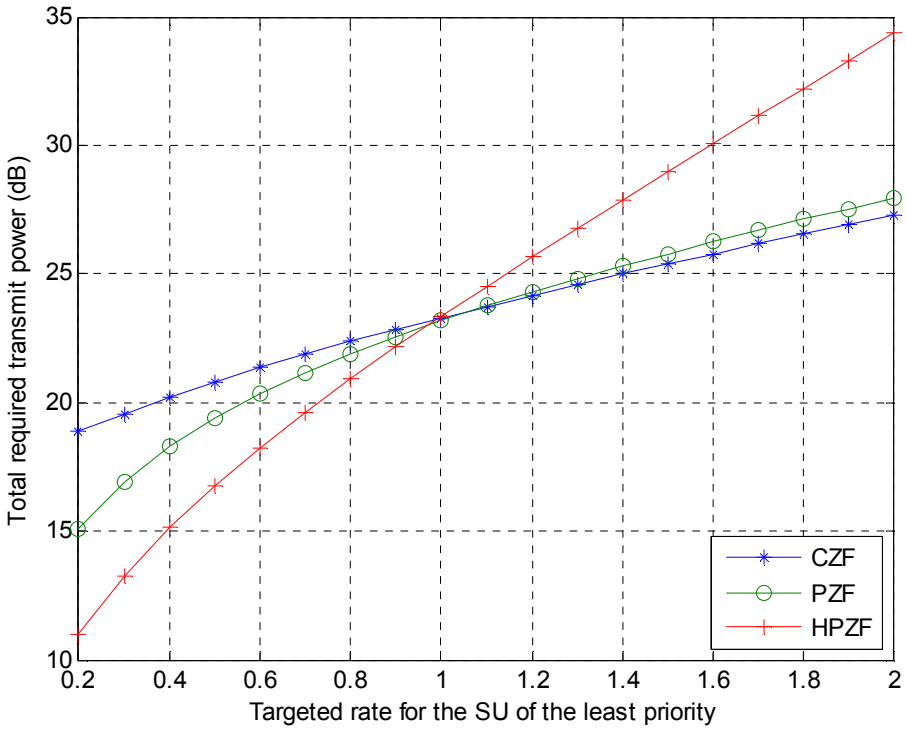

Fig. 3. 17 Comparison of the required transmit power: M=4, L=5, all SUs have the same target rates, $R_p = 1$.

3.8 RESULTS SUMMARY

It can be deduced from the above analytical analysis and/or the simulation results for the case of one PU and 2 SU's:

- When the targeted rates for both 1st SU and 2nd SU are less than 1 bit/sec/Hz, HPZF outperforms the other two schemes.
- When the targeted rate for the 2ndSU is less than 1 bit/sec/Hz, HPZF outperforms PZF whatever the other parameters for the other users are, as was proven analytically before.

CHAPTER 4
CONCLUSION AND FUTURE WORK

4.1 CONCLUSION

Cognitive radio deployment has been proposed to overcome the radio spectrum virtual scarcity problem that is a result of fixed spectrum allocation, which imposes constraints on emerging new wireless applications. In this thesis we have focused on the utilization of MIMO techniques with CR.

In the first part of this thesis, we have considered the spatial spectrum holes detection in an uplink MU-MIMO OFDM scenario and proposed modified spectrum spatial holes sensing algorithms. Optimal and Suboptimal MAP based detectors with relaxed constraints for spectrum spatial holes detection were proposed, which make use of the finite alphabet property along with the a priori activity pattern of PU activity and the OFDM signal block structure. Two environments for a CR were considered where each PU's activity was modeled as a two-state Markov chain. First, static environment where the stationary probability of PU activity is a priori known with no knowledge about the transition probabilities was considered. Second, dynamic environment where the transition probability between the active and inactive states of the PU is a priori known was considered. Simulation results have shown the performance gains of our proposed algorithms with respect to both MMSE detector and the compressive sensing detector previously proposed that is based only on the block sparsity of the OFDM signal [37].

In the second part of this thesis, we have considered the cognitive radio relaying in the physical layer where the cognitive radio base station (CBS) relays the PU signals while transmitting its own signals to its prioritized SUs. We have focused on proposing a new simple linear scheme denoted as hierarchal prior zero forcing (HPZF) scheme, which considers the prioritized issue of users in a CRN. The special case of two SUs was studied. We proved that in the two SUs scenario, the HPZF algorithm outperforms the previously proposed PZF scheme that is only concerned with the PU priority, with respect to the total power requirement as long as the target rate for the least SU is less than 1 bit/sec/Hz. Also, the HPZF and PZF schemes were compared with the CZF scheme, and it was proven that it is

not always guaranteed to find a region for the targeted rates of the SUs where the PZF scheme always requires less total power for achieving each user target rate. Moreover, simulation results were conducted to study the outage performance for each user using the HPZF, PZF and CZF schemes concluding that HPZF gives better outage performance for both the PU and the 1st SU, while the outage performance for the 2nd SU becomes better than using the other schemes if the targeted rate is less than 1 bit/sec/Hz. Also, it was shown that HPZF scheme preserves the outage performance for each user whatever the number of extra SUs entering the CRN is.

4.2 FUTURE WORK

The modified algorithms for spatial holes detection we considered in the first thrust of the thesis could be extended by examining the case where the CBS acts as a decode-and-forward relay for the PUs data. Also, we have considered a perfect channel knowledge model; however, in practical situations there may exist some error in channel estimation, so one possible future work is to examine the effect of channel estimation errors on the performance of our proposed spatial holes detection algorithms and its effect on the PU network as well as the effect of outdated channel estimates.

Regarding the second thrust of the thesis, the newly proposed idea of hierarchal prior zero forcing HPZF scheme could be extended to be studied on cluster level such that each cluster has a group of SUs with the same priority. Another extension could be by considering multiple antennas at the users. Also, studying the allocation of priority to the SUs according to the number of antenna they possess could be considered in the future work, such that the total sum rate is maximized using the HPZF scheme.

REFERENCES

[1] Force, F., "*Report of the Spectrum Efficiency Working Group*," Washington DC, November, 2002.

[2] Ying-Chang Liang; Kwang-Cheng Chen; Li, G.Y.; Mahonen, P., "*Cognitive Radio Networking and Communications: An Overview*," Vehicular Technology, IEEE Transactions on , vol.60, no.7, pp.3386,3407, Sept. 2011.

[3] Qing Zhao; Sadler, B.M., "*A Survey of Dynamic Spectrum Access*," Signal Processing Magazine, IEEE , vol.24, no.3, pp.79,89, May 2007.

[4] Akyildiz, I.F.; Lee, W.Y.; Vuran, M.C.; Mohanty, S., "*Next Generation/Dynamic Spectrum Access/Cognitive Radio Wireless Networks: A Survey*," Computer Networks, vol. 50, no. 13, pp. 2127–2159, 2006.

[5] Yucek, T.; Arslan, H., "*Spectrum Characterization for Opportunistic Cognitive Radio Systems*," Military Communications Conference, 2006. MILCOM 2006. IEEE , vol., no., pp.1,6, 23-25 Oct. 2006.

[6] Yucek, T.; Arslan, H., "*A survey of spectrum sensing algorithms for cognitive radio applications*," Communications Surveys & Tutorials, IEEE , vol.11, no.1, pp.116,130, First Quarter 2009.

[7] Jung-Hoon Noh; Seong-Jun Oh, "*Beamforming in Cognitive Radio with Partial Channel State Information*," Global Telecommunications Conference (GLOBECOM 2011), 2011 IEEE , vol., no., pp.1,6, 5-9 Dec. 2011.

[8] Deepak R. Joshi, " *Spectrum Adaption in Cognitive radio System with Operating Constraints*," Ph.D. Dissertation, Old Dominion University, Dec 2011.

[9] Farhang-Boroujeny, B., "*OFDM Versus Filter Bank Multicarrier*," Signal Processing Magazine, IEEE , vol.28, no.3, pp.92,112, May 2011.

[10] Sampath, H.; Talwar, S.; Tellado, J.; Erceg, V.; Paulraj, A., "*A Fourth Generation MIMO-OFDM Broadband Wireless System: design, Performance, and Field Trial Results*," Communications Magazine, IEEE , vol.40, no.9, pp.143,149, Sep 2002.

[11] Spencer, Q.H.; Peel, C.B.; Swindlehurst, A.L.; Haardt, M., "*An Introduction to the Multi-user MIMO Downlink*," Communications Magazine, IEEE , vol.42, no.10, pp.60,67, Oct. 2004.

[12] Boyd, S.; Vandenberghe, L., Convex Optimization, Cambridge University Press, 2004.

[13] Seung-Jean Kim; Koh, K.; Lustig, M.; Boyd, S.; Gorinevsky, D., "*An Interior-Point Method for Large-Scale ℓ_1-Regularized Least Squares*," Selected Topics in Signal Processing, IEEE Journal of , vol.1, no.4, pp.606,617, Dec. 2007.

[14] Candes, E.J.; Romberg, J.; Tao, T., "*Robust Uncertainty Principles: Exact Signal Reconstruction from Highly Incomplete Frequency Information*," Information Theory, IEEE Transactions on , vol.52, no.2, pp.489,509, Feb. 2006.

[15] ZhiTian; Giannakis, G.B., "Compressed Sensing for Wideband Cognitive Radios," Acoustics, Speech and Signal Processing, 2007. ICASSP 2007. IEEE International Conference on , vol.4, no., pp.IV-1357,IV-1360, 15-20 April 2007.

[16] Wotao Yin; Zaiwen Wen; Shuyi Li; JiaMeng; Zhu Han, "*Dynamic Compressive Spectrum Sensing for Cognitive Radio Networks*," Information Sciences and Systems (CISS), 2011 45th Annual Conference on , vol., no., pp.1,6, 23-25 March 2011.

[17] Eldar, Y.C.; Kuppinger, P.; Bolcskei, H., "*Block-Sparse Signals: Uncertainty Relations and Efficient Recovery*," Signal Processing, IEEE Transactions on , vol.58, no.6, pp.3042,3054, June 2010.

[18] Stojnic, M., " *ℓ_2/ℓ_1-Optimization in Block-Sparse Compressed Sensing and Its Strong Thresholds*," Selected Topics in Signal Processing, IEEE Journal of , vol.4, no.2, pp.350,357, April 2010.

[19] Hao Zhu; Giannakis, G.B., "*Exploiting Sparse User Activity in Multiuser Detection*," Communications, IEEE Transactions on , vol.59, no.2, pp.454,465, February 2011.

[20] Ezzeldin, Y. H.; Sultan, R.; Seddik, K. G., "*Sparse Reconstruction-Based Detection of Spatial Dimension Holes in Cognitive Radio Networks*", accepted for publication in IEEE International Symposium on Personal, Indoor and Mobile Radio Communications (PIMRC), London, UK, Sept. 2013.

[21] Yonghong Zeng; Tung-Sang Ng, "*A Semi-Blind Channel Estimation Method for Multiuser Multiantenna OFDM systems*," Signal Processing, IEEE Transactions on , vol.52, no.5, pp.1419,1429, May 2004.

[22] Csurgai-Horvath, L.; Bito, J., "*Primary and Secondary User Activity Models for Cognitive Wireless Network*," Telecommunications (ConTEL), Proceedings of the 2011 11th International Conference on , vol., no., pp.301,306, 15-17 June 2011.

[23] Akin, S.; Gursoy, M.C., "*Performance Analysis of Cognitive Radio Systems under QoS Constraints and Channel Uncertainty*," Global Telecommunications Conference (GLOBECOM 2010), 2010 IEEE , vol., no., pp.1,5, 6-10 Dec. 2010.

[24] Kae Won Choi; Hossain, E., "*Estimation of Primary User Parameters in Cognitive Radio Systems via Hidden Markov Model*," Signal Processing, IEEE Transactions on , vol.61, no.3, pp.782,795, Feb.1, 2013.

[25] Qian Zhang; JunchengJia; Jin Zhang, "*Cooperative Relay to Improve Diversity in Cognitive Radio Networks*," Communications Magazine, IEEE , vol.47, no.2, pp.111,117, February 2009.

[26] Islam, H.; Ying-Chang Liang; Anh Tuan Hoang, "*Joint Power Control and Beamforming for Cognitive Radio Networks*," Wireless Communications, IEEE Transactions on , vol.7, no.7, pp.2415,2419, July 2008.

[27] Lan Zhang; Ying-Chang Liang; Yan Xin; Poor, H.V., "*Robust Cognitive Beamforming with Partial Channel State Information*," Wireless Communications, IEEE Transactions on , vol.8, no.8, pp.4143,4153, August 2009.

[28] Song, S. H.; Zhang, Q.T., "*Mutual Information of Multipath Channels with Imperfect Channel Information*," Communications, IEEE Transactions on , vol.57, no.5, pp.1523,1531, May 2009.

[29] Gan Zheng; Shaodan Ma; Kai-Kit Wong; Tung-Sang Ng, "*Robust Beamforming in Cognitive Radio*," Wireless Communications, IEEE Transactions on , vol.9, no.2, pp.570,576, February 2010.

[30] Song, S.H.; Hasna, M.O.; Letaief, K.B., "*Prior Zero Forcing for Cognitive Relaying*," Wireless Communications, IEEE Transactions on , vol.12, no.2, pp.938,947, February 2013.

[31] http://www.transition.com/Transition Networks/Uploads/Literature/qos_wp.pdf

[32] Tumuluru, V.K.; Ping Wang; Niyato, D.; Wei Song, "*Performance Analysis of Cognitive Radio Spectrum Access With Prioritized Traffic*," *Vehicular Technology, IEEE Transactions on* , vol.61, no.4, pp.1895,1906, May 2012.

[33] Tigang Jiang; Honggang Wang; Vasilakos, A.V., "*QoE-Driven Channel Allocation Schemes for Multimedia Transmission of Priority-Based Secondary Users over Cognitive Radio Networks*," *Selected Areas in Communications, IEEE Journal on* , vol.30, no.7, pp.1215,1224, August 2012.

[34] Guha, A.; Ganapathy, S.V., *"Power Allocation Schemes for Cognitive Radios," Communication Systems Software and Middleware and Workshops, 2008. COMSWARE 2008. 3rd International Conference on , vol., no., pp.51,56, 6-10 Jan. 2008.*

[35] Motamedi, Norooz; Kumar, Sunil; Hu, Fei; Rowe, Nathaniel, "*A Priority-Aware Channel Selection Scheme for Real-Time Data Transmission in Cognitive Radio Networks*," Computing, Networking and Communications (ICNC), 2013 International Conference on , vol., no., pp.734,739, 28-31 Jan. 2013.

[36] Hamdi, K.; Zarifi, K.; Ben Letaief, K.; Ghrayeb, A., "*Beamforming in Relay-Assisted Cognitive Radio Systems: A Convex Optimization Approach*," Communications (ICC), 2011 IEEE International Conference on , vol., no., pp.1,5, 5-9 June 2011.

[37] Salib, F.; Seddik, K. G., "*Exploiting Spatial Spectrum Holes in Multiuser MIMO systems*", accepted for publication in the 47th Asilomar Conference on Signals, Systems and Computers, Pacific Grove, CA, Nov. 2013.